SID 66-1224

SATELLITE ORBITAL TRANSFER STUDIES
(FINAL REPORT)

Contract No. NAS 8-20238

16 August 1966

Prepared by
Gary A. McCue
David F. Bender

Space Sciences

Approved by

Frank J. Morin
Director

NORTH AMERICAN AVIATION, INC.
SPACE and INFORMATION SYSTEMS DIVISION

2

SID 66-1224

SATELLITE ORBITAL TRANSFER STUDIES
(FINAL REPORT)

Contract No. NAS 8-20238

16 August 1966

Prepared by
Gary A. McCue
David F. Bender

Space Sciences

Approved by

Frank J. Morin
Director

NORTH AMERICAN AVIATION, INC.
SPACE and INFORMATION SYSTEMS DIVISION

FOREWORD

This report is the concluding technical document required under contract NAS8-20238 ("Investigation of Problems of Optimum Satellite Orbital Transfer and Rendezvous").

The work described in this report was performed by the Space Sciences Department of the Space and Information Systems Division, North American Aviation, Inc., during a 14 month period commencing on June 29, 1965 and ending on August 30, 1966.

CONTENTS

ABSTRACT

Quasilinearization was employed to solve two orbital transfer problems. The first involves a discontinuous two-point boundary value problem which resulted from a variational formulation concerning optimal orbital transfer. The boundary conditions were such that the transfer trajectory's end points could be assumed to be at unspecified positions upon arbitrary coplanar orbits. The vehicle was assumed to be thrust limited and capable of controlling thrust direction and duration ("bang-bang" throttle control). Through careful use of the quasilinearization technique it was possible to determine trajectories that minimized the fuel required for orbital transfer maneuvers which were accomplished in a fixed time interval. It was found that accurate initial conditions, which were derived from the corresponding optimal impulsive orbital transfers, were required for convergence of the quasilinearization process. An IBM 7094 double-precision computer program incorporating the above techniques then was utilized to generate optimal transfers between numerous pairs of arbitrary coplanar orbits. Using the resulting data, it was possible to make a series of significant comparisons concerning the velocity changes required for corresponding optimal finite-thrust and optimal impulsive orbital transfers. Further numerical investigations demonstrated the existence of optimal transfers between "shallowly intersecting" orbits which required only one thrusting period. These maneuvers were shown to be analogous to the better known optimal one-impulse maneuver.

The second problem concerned finding impulsive transfers in the general three-body problem. A computer program was developed by employing the quasilinearization technique to solve the two-point boundary value problem that occurs. The specified boundary conditions were the departure point (position and velocity at some point along an initial orbit or trajectory) and the arrival point (position and velocity at some point along a final orbit or trajectory). It was also necessary to specify the transfer time and the general nature of the expected transfer (e.g., forward around the earth to retrograde around the moon). The problem was to find the impulses required to complete the transfer. The required initial estimate of the trajectory was produced by a patched conic trajectory program, but it may also be supplied in as many as ten linear segments.

Unclassified

Satellite Orbital Transfer Studies
(Final Report)

Gary A. McCue and David F. Bender

S&ID - Downey

SID 66-1224

16 August 1966 NAS 8-20238

Orbital Transfer
Quasilinearization
Finite-Thrust
Impulsive Transfer
Boundary Value Problems
Three-Body Problem

Quasilinearization was employed to solve two orbital transfer problems. The first involves a discontinuous two-point boundary value problem which resulted from a variational formulation concerning optimal orbital transfer. The boundary conditions were such that the transfer trajectory's end points could be assumed to be at unspecified positions upon arbitrary coplanar orbits. The vehicle was assumed to be thrust limited and capable of controlling thrust direction and duration ("bang-bang" throttle control). Through careful use of the quasilinearization technique it was possible to determine trajectories that minimized the fuel required for orbital transfer maneuvers which were accomplished in a fixed time interval. It was found that accurate initial conditions, which were derived from the corresponding optimal impulsive orbital transfers, were required for convergence of the quasilinearization process. An IBM 7094 double-precision computer program incorporating the above techniques then was utilized to generate optimal transfers between numerous pairs of arbitrary coplanar orbits. Using the resulting data, it was possible to make a series of significant comparisons concerning the velocity changes required for corresponding optimal finite-thrust and optimal impulsive orbital transfers. Further numerical investigations demonstrated the existence of optimal transfers between "shallowly intersecting" orbits which required only one thrusting period. These maneuvers were shown to be analogous to the better known optimal one-impulse maneuver.

The second problem concerned finding impulsive transfers in the general three-body problem. A computer program was developed by employing the quasilinearization technique to solve the two-point boundary value problem that occurs. The specified boundary conditions were the departure point (position and velocity at some point along an initial orbit or trajectory) and the arrival point (position and velocity at some point along a final orbit or trajectory). It was also necessary to specify the transfer time and the general nature of the expected transfer (e.g., forward around the earth to retrograde around the moon). The problem was to find the impulses required to complete the transfer. The required initial estimate of the trajectory was produced by a patched conic trajectory program, but it may also be supplied in as many as ten linear segments.

INTRODUCTION

During the past seven years the authors have participated in a series of contractual studies of optimal orbital transfer and rendezvous. Under the initial contract, NAS 8-4, work consisted of formulation and parameter studies involving coplanar two-impulse transfer (Refs. 1 to 3). The second contracted effort (NAS 8-1582) was devoted to developing numerical methods for finding the absolute minimum two-impulse transfers between arbitrary non-coplanar non-coapsidal elliptical orbits. This work, which is documented in Refs. 4 to 13, led to several computational methods for solving such problems. The third contract in this series (NAS 8-5211) produced several refinements to the previously successful numerical techniques (Refs. 14 and 15). It also led to the development of a steep descent numerical optimization program (Refs. 16 and 17). Using this numerical program, it was possible to conduct a number of studies which have now been published (Refs. 17, 18, 19 and 20). This contract also produced a variational formulation of the finite thrust optimum orbital transfer problem (Ref. 21). The formulation was programmed for solution using an ordinary Newton-Raphson convergence technique which was later found to be inadequate for this extremely sensitive problem. The results of this third contract are summarized in Ref. 22.

Under the current contract (NAS 8-20238) effort was concentrated upon solving the finite thrust orbital transfer problem and upon an investigation of impulsive transfer in the three-body problem. During the course of the study both of these problems were satisfactorily solved

by employing a mathematical technique known as quasilinearization (Refs. 23, 24 and 25).

This report presents the results of the finite thrust orbital transfer study as Appendix A. Appendix A was previously distributed as a separate document (Ref. 26). Appendix B contains a separate paper describing the formulation and computer program utilized to produce two-impulse transfer circumstances in the three-body problem. Initial conditions for this problem were obtained from a patched conic trajectory program which was also developed as part of this contract effort.

During the past year it was also possible to update and revise several of the computer programs for performing numerical studies of two-impulse transfers in the two-body problem. These programs have now been documented and are available for use (Refs. 16, 27, 28 and 29).

RESULTS OF STUDY

The numerical results demonstrated that quasilinearization is a powerful tool for the optimization of two-point boundary value problems. This was true of both the two-body finite thrust and the three-body impulsive transfer studies. In the two-body problem, it was found that impulsive results offered a good first approximation to their finite thrust counterparts. For this reason, it was possible to fully utilize prior impulsive orbital transfer studies when generating finite thrust trajectories about a single attracting center. This result also implies that the impulsive three-body trajectories would be excellent first approximations when seeking their finite thrust counterparts. Complete details of this work appears as Appendices A and B.

The success of these studies strongly suggests that this work should be expanded to include a three-dimensional formulation of the finite thrust orbital transfer problem. Also, the three-body work should be expanded to include a finite thrust formulation in three dimensions. In both instances, the results and computer programs generated under the current study should prove invaluable.

REFERENCES

1. Kerfoot, H.P. and DesJardins P.R., "Analytical Study of Satellite Rendezvous", North American Aviation, Inc., MD 59-462, (January 1960).
2. Kerfoot, H.P., Bender, D.F., and DesJardins, P.R., "Analytical Study of Satellite Rendezvous" (Final Report), North American Aviation, Inc., MD 59-272, (20 October 1960).
3. Kerfoot, H.P. and DesJardins, P.R., "Co-Planar Two-Impulse Orbital Transfers," ARS Pre-print 2063-61, (9 October 1961).
4. DesJardins, P.R. and Bender, D.F., "Extended Satellite Rendezvous Study" (Quarterly Report), North American Aviation, Inc., SID 61-304, (14 September 1961).
5. DesJardins, P.R. and Bender, D.F., "Satellite Rendezvous Study" (Second Quarterly Report), North American Aviation, Inc., SID 61-459, (15 December 1961).
6. DesJardins, P.R. and Bender, D.F., "Satellite Rendezvous Study" (Third Quarterly Report), North American Aviation, Inc., SID 62-339, (15 March 1962).
7. DesJardins, P.R., Bender, D.F., and McCue, G.A., "Orbital Transfer and Satellite Rendezvous" (Final Report), North American Aviation, Inc., SID 62-870, (31 August 1962).
8. Bender, D.F., "Optimum Co-Planar Two-Impulse Transfers Between Elliptic Orbits," Aerospace Engineering, No. 10, p. 44 (October 1962).

9. Bender, D.F., "Rendezvous Possibilities With the Impulse of Optimum Two-Impulse Transfer," Advancements in Astronautical Sciences (AAS), Vol. 16 (Part One), pp. 271-291 (1963). (Published in "Progress Report #3 on Studies in the Fields of Space Flight and Guidance Theory," MSFC, NASA, Huntsville, Alabama, pp. 138-153, 6 February 1963).

10. McCue, G.A., "Visualization of Functions by Stereographic Techniques," North American Aviation, Inc., SID 63-170, (20 January 1963).

11. McCue, G.A., "Optimization by Function Contouring Techniques," North American Aviation, Inc., SID 63-171, (10 February 1963). (Presented at 1963 ACM Conference, 27 August 1963).

12. McCue, G.A., "Optimum Two-Impulse Orbital Transfer and Rendezvous Between Inclined Elliptical Orbits," AIAA Journal, Vol. 1, No. 8, August 1963. (Presented at AIAA Astrodynamics Conference, 20 August 1963. Published in "Progress Report #4 on Studies in the Fields of Space Flight and Guidance Theory," MSFC, NASA, Huntsville, Alabama, September 1963).

13. McCue, G.A., "Optimization and Visualization of Functions," AIAA Journal, Vol. 2, No. 1, (January 1964).

14. Lee, G., "An Analysis of Two-Impulse Orbital Transfer," AIAA J., 2, 1767-1173 (1964). (Published in "Progress Report #4 on Studies in the Fields of Space Flight and Guidance Theory," MSFC, NASA, Huntsville, Alabama, pp. 167-212, 19 September 1963).

15. Lee, G., "On a Restricted Comparison of Two-Impulse and One-Impulse Orbital Transfer," North American Aviation, Inc., SID 63-1026, (Published in "Progress Report #5 on Studies in the Fields of Space Flight and Guidance Theory," MSFC, NASA, Huntsville, Alabama, 19 September 1963).

16. McCue, G.A., and Hoy, R.C., "Optimum Two-Impulse Orbital Transfer Program," North American Aviation, Inc., SID 65-1119, (1 August 1965).

17. McCue, G.A., and Bender, D.F., "Numerical Investigation of Minimum Impulse Orbital Transfer," AIAA J., 3, 2328-2334 (December 1965).

18. McCue, G.A., and Bender, D.F., "Optimum Transfers Between Nearly Tangent Orbits," AAS J., Vol. 13, No. 2, (March-April 1966).

19. Bender, D.F. and McCue, G.A., "Conditions for Optimal One-Impulse Transfer," North American Aviation, Inc., SID 64-1859 (1 October 1964).

20. Bender, D.F., "A Comparison of One- and Two-Impulse Transfer for Nearly Tangent Co-Planar Orbits," (Published in "Progress Report #5 on Studies in the Fields of Space Flight and Guidance Theory," MSFC, NASA, Huntsville, Alabama, (19 September 1963).

21. Jurovics, S.A., "Orbital Transfer by Optimum Thrust Direction and Duration," North American Aviation, Inc., SID 64-29, (12 February 1964).

22. McCue, G.A., Bender, D.F., and Jurovics, S.A., "Satellite Rendezvous Study Summary Report," North American Aviation, Inc., SID 64-368, (10 March 1964).

23. Kalaba, R., Some Aspects of Quasilinearization, (Nonlinear Differential Equations and Non linear Mechanics) New York; Academic Press, Inc., pp. 135-146 (1963).

24. Bellman, R., Kagiwada, H., and Kalaba, R., "Quasilinearization, System Identification and Prediction," RAND CORP., RM - 3812 PR (August 1963).

25. McGill, R. and Kenneth, P., "Solution of Variational Problems by Means of a Generalized Newton-Raphson Operator," AIAA J., 2, pp. 1761-1766 (October 1964).

26. McCue, G.A., "Quasilinearization Determination of Optimum Finite-Thrust Orbital Transfers," North American Aviation, Inc., SID 66-1278, (29 July 1966).

27. McCue, G.A., and DuPrie, H.J., "Optimum Two-Impulse Orbital Transfer Function Contouring Program," North American Aviation, Inc., SID 65-1181 (1 September 1965).

28. McCue, G.A., Dworetsky, M. and DuPrie, H.J., "Fortran IV Stereographic Function Representation and Contouring Program," North American Aviation, Inc., SID 65-1182 (1 September 1965).

29. McCue, G.A. and DuPrie, H.J., "Improved Fortran IV Function Contouring Program," North American Aviation, Inc., SID 65-672, (1 April 1965).

APPENDIX A*

QUASILINEARIZATION DETERMINATION OF OPTIMUM FINITE-THRUST ORBITAL TRANSFERS

*Note that this appendix is a separate paper having its own nomenclature, illustrations, references, etc.

CONTENTS

NOMENCLATURE

A	First Integral
$\underset{\sim}{B}$	Boundary Condition Vector
c	Effective Exhaust Velocity
C_j	Combination Coefficients Required for Quasilinearization Process
D	Auxiliary Variable Defined by Equation 26
e	Eccentricity
F	Thrust
G	Quantity to be Minimized (Maximized)
$\underset{\sim}{H}_j$	Homogeneous Solution Vectors Required for Quasilinearization Process
$\underset{\sim}{g}$	Time Derivative Vector
k	Switching Function
m	Mass
N	Number of Differential Equations
n	Quasilinearization Iteration Number
$\underset{\sim}{P}$	Particular Solution Vector Required for Quasilinearization Process
p	Semilatus Rectum
r	Radius
T	Total Time Required for Transfer Maneuver
t	Time
$\underset{\sim}{X}$	Dependent Variable Vector

x	Components of Vector X
y	Angular Velocity (ϕ)
β	Mass Flow Rate
ϕ	Central Angle
λ_i	Lagrange Multiplier
ρ	Radial Velocity
μ	Gravitational Constant
ν	Steering Angle
ω	Argument of Perigee

ILLUSTRATIONS

ABSTRACT

Quasilinearization was utilized to solve a discontinuous two-point boundary value problem which resulted from a variational formulation concerning optimal orbital transfer. The boundary conditions were such that the transfer trajectory's end points could be assumed to be at unspecified positions upon arbitrary coplanar orbits. The vehicle was assumed to be thrust limited and capable of controlling thrust direction and duration ("bang-bang" throttle control). Through careful use of the quasilinearization technique it was possible to determine trajectories that minimized the fuel required for orbital transfer maneuvers which were accomplished in a fixed time interval. It was found that accurate initial conditions, which were derived from the corresponding optimal impulsive orbital transfers, were required for convergence of the quasilinearization process. An IBM 7094 double-precision computer program incorporating the above techniques then was utilized to generate optimal transfers between numerous pairs of arbitrary coplanar orbits. Using the resulting data, it was possible to make a series of significant comparisons concerning the velocity changes required for corresponding optimal finite-thrust and optimal impulsive orbital transfers. Further numerical investigations demonstrated the existence of optimal transfers between "shallowly intersecting" orbits which required only one thrusting period. These maneuvers were shown to be analogous to the better known optimal one-impulse maneuver.

I. INTRODUCTION

Certain realistic treatments of the optimum orbital transfer problem lead to a variational formulation wherein the differential equations have no exact closed form solution. Prior experience with the particular two point boundary value problem considered here[1] indicated that it was extremely sensitive and could not be solved by an ordinary Newton-Raphson method. Reformulation and application of "quasilinearization"[2,3,4] allowed the successful computation of optimal "finite-thrust" transfer trajectories between arbitrary pairs of coplanar elliptical orbits. However, successful application of quasilinearization was found to depend upon the proper use of initial conditions derived from an optimum two-impulse transfer maneuver.[5,6,7,8]

II. THE OPTIMIZATION PROBLEM

The problem to be considered here involves transferring between a pair of coplanar orbits defined by their semi-latera recta (p_1,p_2), eccentricities (e_1,e_2) and arguments of perigee (ω_1,ω_2). What is required is the determination of that trajectory which results in an orbital transfer with minimum fuel expenditure. The formulation is a modified version of a three-dimensional derivation originated by Jurovics[1] and is similar to that presented by Leitmann.[9] Solution of this optimization problem involves the minimization of a functional which is a function of only the boundary values of the state variables: i.e. position, velocity, mass and time.

The function to be minimized is the characteristic velocity:

$$G = c \ln \frac{m_0}{m_T} \tag{1}$$

where,

$$G = G(x_{i0},x_{iT}) \tag{2}$$

and, where the state variables are:

$$x_i = r, \phi, \dot{r}, \dot{\phi}, m \tag{3}$$

In the above expressions c = effective exhaust velocity; r = radius, ϕ = central angle; m = mass, and the subscripts 0 and T refer to initial and final points of the trajectory.

The rocket and its environment are defined in accordance with the following assumptions:

1. The rocket is a variable mass particle.

2. The thrust magnitude (F) is a linear function of the mass flow rate (β):

$$F = c\beta = -c\dot{m} \tag{4}$$

3. The vehicle is capable of thrust direction and throttle control, and the control is instantaneous.

4. Further, the transfer maneuver is between two orbits about a single planet with a spherically symmetrical central gravitational field.

EQUATIONS OF MOTION

In polar coordinates (Figure 1), the two second order equations of motion are:

$$\ddot{r} - r\dot{\phi}^2 + \frac{\mu}{r^2} = \frac{F}{m}\cos\nu \tag{5}$$

$$r\ddot{\phi} + 2\dot{r}\dot{\phi} = \frac{F}{m}\sin\nu \tag{6}$$

where,

μ = gravitational constant

ν = steering angle measured from local vertical

These equations may be reduced to first order form, where the new variables ρ and y are defined as follows:

$$\rho = \dot{r} \tag{7}$$

$$y = \dot{\phi} \tag{8}$$

$$\dot{\rho} = ry^2 - \frac{\mu}{r^2} + \frac{c\beta}{m}\cos\nu \tag{9}$$

$$\dot{y} = -\frac{2\rho y}{r} + \frac{c\beta}{mr}\sin\nu \tag{10}$$

$$\dot{m} = -\beta \tag{11}$$

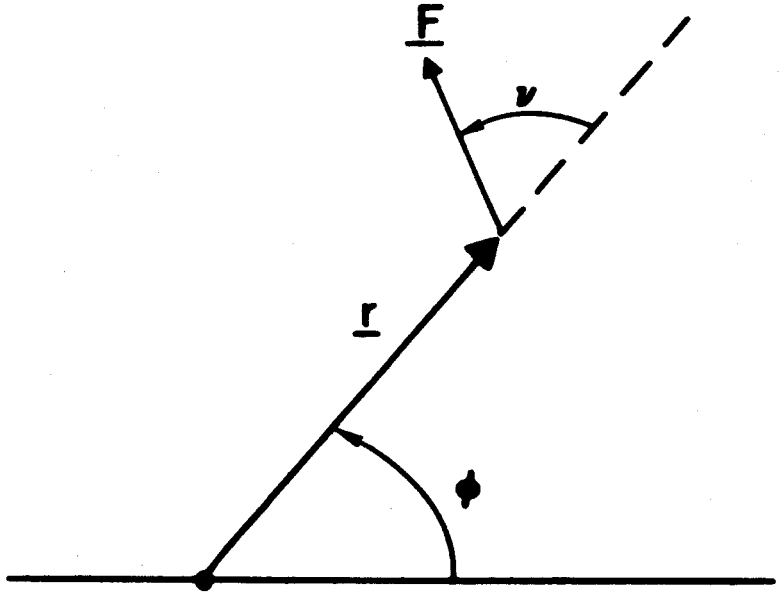

Figure 1 - Coordinate System Definition

EULER LAGRANGE EQUATIONS

The optimum path must satisfy the above equations of motion. In addition, for most conventional rockets, the solution is subject to the following constraints:

$$c = \text{constant} \tag{12}$$

$$\beta_{min} \leq \beta \leq \beta_{max} \tag{13}$$

where $\beta_{min} = 0$, and β_{max} is specified.

In the problem considered here one utilizes the following additional constraint to impose "bang-bang" control of mass flow rate:

$$\beta(\beta - \beta_{max}) = 0 \tag{14}$$

If G is to possess an extremum subject to the constraints imposed by Equations 7 to 12 and 14, one must require the first variation of the constrained functional to vanish. The following Euler-Lagrange differential equations for the Lagrange multipliers result:

$$\dot{\lambda}_1 = -\lambda_4\left(y^2 + \frac{2\mu}{r^3}\right) - \lambda_6\left(\frac{2\rho y}{r^2} - \frac{c\beta \sin \nu}{mr^2}\right) \tag{15}$$

$$\dot{\lambda}_3 = 0 \tag{16}$$

$$\dot{\lambda}_4 = -\lambda_1 + \frac{2\lambda_6 y}{r} \tag{17}$$

$$\dot{\lambda}_6 = -\lambda_3 - 2\lambda_4 ry + \frac{2\lambda_6 \rho}{r} \tag{18}$$

$$\dot{\lambda}_7 = \frac{c\beta}{m^2}\left[\lambda_4 \cos \nu + \frac{\lambda_6 \sin \nu}{r}\right] \tag{19}$$

The differential equation for λ_7 also may be written in the following useful form:

$$\dot{\lambda}_7 = \frac{\beta}{m}\left|k + \lambda_7\right| \tag{20}$$

The "switching function" (k), which appears in Equation 20, governs thrust on-off control and is defined as follows:

$$k = \frac{c}{m} \left(\lambda_4 \cos \nu + \frac{\lambda_6 \sin \nu}{r} \right) - \lambda_7 \tag{21}$$

where,

$$k > 0 \Rightarrow \beta = \beta_{max} \tag{22}$$

$$k < 0 \Rightarrow \beta = 0 \tag{23}$$

Equations for the steering angle (ν) are as follows:

$$\sin \nu = \frac{\lambda_6}{D} \tag{24}$$

$$\cos \nu = \frac{\lambda_4 r}{D} \tag{25}$$

where,

$$D = \sqrt{\lambda_6^2 + \lambda_4^2 r^2} \tag{26}$$

Clearly, the steering angle has no physical significance when the vehicle is on a coasting arc.

Since the differential equations do not involve time explicitly, one obtains a first integral (Hamiltonian):

$$\lambda_1 \dot{r} + \lambda_3 \dot{\phi} + \lambda_4 \dot{\rho} + \lambda_6 \dot{y} + \lambda_7 \dot{m} = A \tag{27}$$

where,

$$A = \text{constant} \tag{28}$$

These last expressions may be used to replace one of the Euler-Lagrange differential equations and thereby reduce the order of the system by one.

BOUNDARY CONDITIONS

Note that the system is described by 10 equations for the variables:

$$r, \phi, \rho, y, m, \lambda_1, \lambda_3, \lambda_4, \lambda_6, \lambda_7$$

This system thus requires 10 boundary conditions. The seven specified by the physics of the problem are:

$$p_1, e_1, \omega_1, p_2, e_2, \omega_2, m_0$$

The remaining boundary conditions can be derived from the transversality condition:

$$dG + \left[\lambda_1 dr + \lambda_3 d\phi + \lambda_4 d\rho + \lambda_6 dy + \lambda_7 dm - A dt \right]_0^T = 0 \qquad (29)$$

One may then obtain the following additional boundary conditions:(1)

$$\lambda_7 = \frac{c}{m} \quad , \quad t = T \qquad (30)$$

$$\left[\lambda_1 dr + \lambda_3 d\phi + \lambda_4 d\rho + \lambda_6 dy \right]_0^T = 0 \qquad (31)$$

A somewhat different form of Equation 27 may also be derived:(1)

$$\left[\dot{r}\lambda_1 + \dot{\phi}\lambda_3 + \dot{\rho}\lambda_4 \quad \dot{y}\lambda_6 + \dot{m}\lambda_7 \right]_0^T = \beta k \qquad (32)$$

From this form of the equation, it is clear that the Hamiltonian (A in Equation 20) must be equal to βk at the end points. Further, if $A \neq 0$ at $t = 0$, then Equation 24 implies that $k(0) = k(T)$.

Having obtained a system of 10 first-order ordinary differential equations which must yield the required optimal trajectory over a specified time interval, one next observes that the problem is of mixed end-value nature and only the five values of the state variables are known at the initial point (or final point). However, it is well known that the λ_i can be scaled by a positive constant.(9) Thus, by assigning an appropriate initial value to λ_1, the number of unknown initial conditions was reduced to four.

CORNER CONDITIONS

For this particular problem, the corner conditions are such that the multipliers associated with each of the state variables and A, the first integral, must have the same value immediately preceeding and following a corner.

$$\left(\lambda_i\right)_- = \left(\lambda_i\right)_+ \tag{33}$$

$$A- = A+ \tag{34}$$

III. QUASILINEARIZATION

Having obtained a nonlinear two-point boundary value problem, the powerful method of quasilinearization[2] may be used to generate the required numerical solutions. The previously derived differential equations may be written as a set of ten first-order equations, each of which may be considered to be one component of the vector equation:

$$\dot{\underset{\sim}{X}} = \underset{\sim}{g}\,(\underset{\sim}{X}) \tag{35}$$

where,

$$\underset{\sim}{X} = \begin{bmatrix} r \\ \phi \\ \rho \\ y \\ m \\ \lambda_1 \\ k \\ \lambda_4 \\ \lambda_6 \\ \lambda_3 \end{bmatrix}, \quad \underset{\sim}{g} = \begin{bmatrix} \rho \\ y \\ ry^2 - \frac{\mu}{r^2} + \frac{c\beta}{m}\cos\nu \\ -\frac{2\rho y}{r} + \frac{c\beta}{mr}\sin\nu \\ -\beta \\ -\lambda_4\left(y^2 + \frac{2\mu}{r^3}\right) - \lambda_6\left(\frac{2\rho y}{r^2} - \frac{c\beta}{mr^2}\sin\nu\right) \\ -\frac{c}{mD}\left(r\lambda_1\lambda_4 + \frac{\lambda_3\lambda_6}{r} - \frac{\rho\lambda_6^2}{r^2}\right) \\ -\lambda_1 + \frac{2\lambda_6 y}{r} \\ -\lambda_3 - 2\lambda_4 ry + \frac{2\lambda_6\rho}{r} \\ 0 \end{bmatrix} \tag{36}$$

Note that in the above equations an expression for the switching function (k) has been derived from Equation 20 and substituted for λ_7. This substitution was useful since it replaced an unknown function with one with properties partially defined by the optimum two-impulse transfer maneuver. Since λ_3 is constant throughout a given trajectory it may be regarded as a parameter whose time history may be obtained without resorting to numerical integration. In order to achieve computational economies the computer program required that λ_3 be assigned to the last position in the vectors of Equation 36.

The quasilinearization method may be regarded as an extension of the Newton-Raphson method for algebraic equations to ordinary differential equations. Suppose that the "n'th" approximation to the time history of the solution vector, $\underset{\sim}{X}^{(n)}(t)$ is known. A Taylor series expansion about this approximation, truncated with linear terms, may then be made to obtain the derivative of the (n + 1)st approximation, $\dot{\underset{\sim}{X}}^{(n+1)}$:

$$\dot{x}_i^{(n+1)} = g_i(\underset{\sim}{X}^{(n)}) + \sum_{j=1}^{N} \left[x_j^{(n+1)} - x_j^{(n)}\right] \frac{\partial g_i(\underset{\sim}{X}^{(n)})}{\partial x_j} \qquad (37)$$

$$i = 1, 2 \ldots N$$

where N is the number of differential equations. This is the fundamental equation of quasilinearization.[2,3] In this case the Jacobian matrix of partial derivatives is rather involved (Eq.38, Fig.2). The more lengthy partial derivatives appearing in the Jacobian matrix appear as Equations 39.

$$\left[\frac{\partial g_i}{\partial x_j}\right] = \begin{bmatrix}
0 & 0 & 1 & 0 & 0 & 0 & 0 & 0 & 0 & 0 \\
0 & 0 & 0 & 1 & 0 & 0 & 0 & 0 & 0 & 0 \\
\frac{\partial \dot{\rho}}{\partial r} & 0 & 0 & 2ry & -\frac{c\beta\lambda_4 r}{m^2 D} & 0 & 0 & \frac{c\beta r \lambda_6^2}{m D^3} & -\frac{c\beta r \lambda_4 \lambda_6}{m D^3} & 0 \\
\frac{\partial \dot{y}}{\partial r} & 0 & -\frac{2y}{r} & -\frac{2\rho}{r} & -\frac{c\beta\lambda_6}{m^2 r D} & 0 & 0 & -\frac{c\beta r \lambda_4 \lambda_6}{m D^3} & \frac{c\beta r \lambda_4^2}{m D^3} & 0 \\
0 & 0 & 0 & 0 & 0 & 0 & 0 & 0 & 0 & 0 \\
\frac{\partial \dot{\lambda}_1}{\partial r} & 0 & -\frac{2y\lambda_6}{r^2} & \frac{\partial \dot{\lambda}_1}{\partial y} & -\frac{c\beta\lambda_6^2}{m^2 r^2 D} & 0 & 0 & \frac{\partial \dot{\lambda}_1}{\partial \lambda_4} & \frac{\partial \dot{\lambda}_1}{\partial \lambda_6} & 0 \\
\frac{\partial \dot{k}}{\partial r} & 0 & \frac{c\lambda_6^2}{mDr^2} & 0 & \frac{\partial \dot{k}}{\partial m} & -\frac{c\lambda_4 r}{mD} & 0 & \frac{\partial \dot{k}}{\partial \lambda_4} & \frac{\partial \dot{k}}{\partial \lambda_6} & \frac{-c\lambda_6}{rmD} \\
-\frac{2\lambda_6 y}{r^2} & 0 & 0 & \frac{2\lambda_6}{r} & 0 & -1 & 0 & 0 & \frac{2y}{r} & 0 \\
-2\lambda_4 y - \frac{2\lambda_6 \rho}{r^2} & 0 & \frac{2\lambda_6}{r} & -2\lambda_4 r & 0 & 0 & 0 & -2ry & \frac{2\rho}{r} & -1 \\
0 & 0 & 0 & 0 & 0 & 0 & 0 & 0 & 0 & 0
\end{bmatrix} \tag{38}$$

Figure 2 - Jacobian Matrix (Equation 38)

$$\frac{\partial \dot{\rho}}{\partial r} = y^2 + \frac{2\mu}{r^3} + \frac{c\beta\lambda_4\lambda_6^2}{mD^3}$$

$$\frac{\partial \dot{y}}{\partial r} = \frac{2\rho y}{r^2} - \frac{c\beta\lambda_6}{mr^2D}\left(1 + \frac{r^2\lambda_4^2}{D^2}\right)$$

$$\frac{2\dot{\lambda}_1}{\partial r} = \frac{6\mu\lambda_4}{r^4} + \frac{4\rho y\lambda_6}{r^3} - \frac{c\beta\lambda_6^2}{mr^3D}\left(2 + \frac{r^2\lambda_4^2}{D^2}\right)$$

$$\frac{\partial \dot{k}}{\partial r} = \frac{c}{mD}\left[\frac{\lambda_3\lambda_6}{r^2} - \frac{2\rho\lambda_6^2}{r^3} - \frac{1}{D^2}\left(\lambda_1\lambda_4\lambda_6^2 - \lambda_3\lambda_4^2\lambda_6 + \frac{\rho\lambda_4^2\lambda_6^2}{r}\right)\right]$$

$$\frac{\partial \dot{\lambda}_1}{\partial y} = 2y\lambda_4 - \frac{2\rho\lambda_6}{r^2}$$

$$\frac{\partial \dot{k}}{\partial m} = \frac{c}{m^2D}\left(r\lambda_1\lambda_4 + \frac{\lambda_3\lambda_6}{r} - \frac{\rho\lambda_6^2}{r^2}\right) \qquad (39)$$

$$\frac{\partial \dot{\lambda}_1}{\partial \lambda_4} = -y^2 - 2\frac{\mu}{r^3} - \frac{c\beta\lambda_6^2\lambda_4}{mD^3}$$

$$\frac{\partial \dot{k}}{\partial \lambda_4} = \frac{c\lambda_6}{mD^3}\left(-r\lambda_1\lambda_6 + r\lambda_3\lambda_4 - \rho\lambda_4\lambda_6\right)$$

$$\frac{\partial \dot{\lambda}_1}{\partial \lambda_6} = \frac{-2\rho y}{r^2} + \frac{c\beta\lambda_6}{mr^2D}\left(2 - \frac{\lambda_6^2}{D^2}\right)$$

$$\frac{\partial \dot{k}}{\partial \lambda_6} = \frac{c}{mD^3}\left(-r\lambda_3\lambda_4^2 + \frac{\rho\lambda_6^3}{r^2} + 2\rho\lambda_6\lambda_4^2 + r\lambda_6\lambda_1\lambda_4\right)$$

Because Equation 37 is linear in the $x_i^{(n+1)}$, solutions may be added to satisfy all the boundary conditions. By requiring a particular solution to satisfy the known initial boundary conditions, it is necessary to generate a particular solution (P_i) plus as many homogeneous solutions (H_{ij}) as there are unknown initial boundary conditions (B_i). The correct number of equations to solve for the combination coefficients, C_j, in the remaining four boundary conditions are thus obtained:

$$B_i(T) - P_i(T) = \sum_{j=1}^{4} C_j H_{ij}(T) \quad , \quad i = 1, 2, 3, 4 \tag{40}$$

The (n+1)st approximation, $x_i^{(n+1)}(t)$, is evaluated by summing the stored values of P_i and H_{ij}:

$$x_i^{(n+1)}(t) = P_i(t) + \sum_{j=1}^{4} C_j H_{ij}(t) \; ; \quad i = 1, 2 \ldots . N \tag{41}$$

If the process converges it will do so quadratically.[2,3] However, in order for the process to converge, one must have a sufficiently accurate first approximation, $\underset{\sim}{X}^{(0)}(t)$, to the time history of the solution vector. Convergence of the process may be examined by evaluating the following relationships at the end of each iteration:

$$\xi_i(\underset{\sim}{X}^{(n)} , \underset{\sim}{X}^{(n+1)}) = \underset{t}{MAX} \left| x_i^{(n)}(t) - x_i^{(n+1)}(t) \right| \tag{42}$$

$$i = 1, 2 \ldots . N$$

The abrupt changes in mass flow rate require special consideration. Whenever the switching function exhibits a zero ("switch point") the mass flow rate ($\dot{m} = -\beta$) must undergo a discontinuous change. This property

can be expressed by employing a unit step function in the definition of β:(10)

$$\beta = \beta_0 u \left[k^{(n)}(t) \right] \tag{43}$$

where,

$$u \left[k^{(n)}(t) \right] = \int_{k-}^{k+} \delta \left[k^{(n)}(t) \right] \, dk \tag{44}$$

At a switch point ($k^{(n)} = 0$, and $t = t_s$) Equation 37 must be integrated as follows:

$$\int_{t_{s-}}^{t_{s+}} \dot{x}_i^{(n+1)} dt = \int_{t_{s-}}^{t_{s+}} \left\{ g_i(\underset{\sim}{X}^{(n)}) + \sum_{j=1}^{N} \left[x_j^{(n+1)} - x_j^{(n)} \right] \frac{\partial g_i(\underset{\sim}{X}^{(n)})}{\partial x_j} \right\} dt \tag{45}$$

$$i = 1, 2 \ldots N$$

The $g_i(\underset{\sim}{X}^{(n)})$ term offers no net contribution and may therefore be excluded from further consideration. Next, observe that at a switch point the Jacobian matrix will have some non-zero terms appearing in the column containing partial derivatives with respect to the switching function (k). Note that this is only true at the switch points and that Equation 38 is valid elsewhere. Thus, Equation 45 becomes:

$$\Delta x_i^{(n+1)} = \int_{t_{s-}}^{t_{s+}} \left[k^{(n+1)} - k^{(n)} \right] \frac{\partial g_i(\underset{\sim}{X}^{(n)})}{\partial k} \, dt \tag{46}$$

$$i = 1, 2 \ldots . N$$

Since the switching time is determined by the n'th iteration wherein $k^{(n)} = 0$ one obtains:

$$\Delta x_i^{(n+1)} = \int_{t_{s-}}^{t_{s+}} k^{(n+1)} \frac{\partial g_i(\underset{\sim}{X}^{(n)})}{\partial k} \, dt, \quad i = 1, 2 \ldots N \tag{47}$$

At this point it should be noted that only those terms in Equation 36 which contain mass flow rate will contribute to the solution at a discontinuity. Substitution of Equations 36, 43 and 44 into Equation 47 yields expressions of the following form:

$$\Delta x_i^{(n+1)} = S_i \beta_0 k^{(n+1)} \int_{t_{s-}}^{t_{s+}} \frac{\partial}{\partial k} \int_{k-}^{k+} \delta \left[k^{(n)}(t) \right] dk \, dt \qquad (48)$$

or,

$$\Delta x_i^{(n+1)} = S_i \beta_0 k^{(n+1)} \int_{t_{s-}}^{t_{s+}} \delta \left[k^{(n)}(t) \right] dt, \; i = 1,2...N \qquad (49)$$

where the S_i represent arbitrary constants.

In order to integrate with respect to the argument of the delta function one may adopt the following definitions:

$$k = F(t) , \quad t = F^{-1}(k) \qquad (50)$$

$$dt = \frac{d}{dk} F^{-1}(k) \, dk$$

Equation 49 may now be rewritten and integrated with respect to k;

$$\Delta x_i^{(n+1)} = S_i \beta_0 k^{(n+1)} \int_{k-}^{k+} \delta \left[k^{(n)}(t) \right] \frac{d}{dk} F^{-1}(k) \, dk \qquad (51)$$

$$\Delta x_i^{(n+1)} = S_i \beta_0 k^{(n+1)} \frac{dt}{dk} \int_{k-}^{k+} \delta \left[k^{(n)}(t) \right] dk \qquad (52)$$

$$\Delta x_i^{(n+1)} = S_i \beta_0 k^{(n+1)} / \dot{k} , \quad i = 1, 2....N \qquad (53)$$

Equation 53 now may be applied to derive the following final expressions for the contributions to the solution at a corner point:

$$\Delta\rho = \Delta t \frac{c\beta}{m} \cos \nu \tag{54}$$

$$\Delta y = \Delta t \frac{c\beta}{mr} \sin \nu \tag{55}$$

$$\Delta m = -\beta \Delta t \tag{56}$$

$$\Delta\lambda_1 = \Delta t \frac{c\beta\lambda_6}{mr^2} \sin \nu \tag{57}$$

where,

$$\Delta t = \frac{k^{(n+1)}}{|\dot{k}|} \tag{58}$$

During the integration of the particular and homogeneous solutions required by Equation 40, $k^{(n+1)}$ will, in general, be non-zero at the switch points determined from the n'th iteration. The quantity, Δt, defined in Equation 58 may be regarded as an incremental change in the length of a burn period called for since $k^{(n+1)}$ is now non-zero at the switch points. The incremental changes defined by Equations 54 to 57 compensate for the changes which will result from these small changes in burning time. The need for the absolute value sign can be established by considering the physical implications of a non-zero value of $k^{(n+1)}$ at points where $k^{(n)} = 0$.

IV. NUMERICAL SOLUTION BY QUASILINEARIZATION

COMPUTATION TECHNIQUES

Equations 1 to 58 were programmed in FORTRAN IV for solution by an IBM 7094 digital computer. A double precision integration program (Ref. 11) employing Runge-Cutta starting procedures and a variable step-size difference integration scheme was utilized. The current approximation to the solution, $\underset{\sim}{X}^{(n)}$, as well as $\underset{\sim}{P}$ and the $\underset{\sim}{H}_j$, were generated by integration and stored at fixed tabular intervals. During the integration it was necessary to determine values of the variables between the tabular points. These intermediate values were obtained by Sterling interpolation[12] truncated with second differences. The fifty equations for $\underset{\sim}{P}$ and the $\underset{\sim}{H}_j$ were integrated simultaneously, requiring only one evaluation of g_i and the Jacobian matrix at each value of time (t). After the integration was terminated at the final time (T) the combination coefficients, C_j, were evaluated from Equation (40), and the stored values substituted into Equation (41) to obtain the new approximation: $\underset{\sim}{X}^{(n+1)}$.

Computation was saved by relaxing truncation error requirements where possible. At the beginning of each iteration the best available initial conditions were used for $\underset{\sim}{P}$. The contributions of the $\underset{\sim}{H}_j$ to $\underset{\sim}{X}^{(n+1)}$ therefore diminished as the process converged. Thus, the accuracies of the $\underset{\sim}{H}_j$ were not as important as that of $\underset{\sim}{P}$.

Convergence of the quasilinearization process was tested by comparing the values of $x_i^{(n)}$ and $x_i^{(n+1)}$ at the storage interval according to Equation 42. The entire process described above was performed by

a general purpose quasilinearization subroutine which utilized double-precision FORTRAN IV.[11]

INITIAL CONDITIONS

The extreme sensitivity of the orbital transfer maneuvers considered here was promptly discovered. For instance, small changes in the durations of the thrust periods were found to produce large variations in the trajectory. Such small variations would often cause the process to diverge. It was therefore necessary to obtain a realistic approximation to the optimal trajectory prior to the initiation of the quasilinearization computations.

It was found that the optimum two-impulse orbital transfer yielded an excellent initial approximation to its finite thrust counterpart. Accordingly, an initial conditions subroutine which utilized a steep descent numerical optimization program (Refs. 8 and 13) was employed to generate an initial approximation to the trajectory: $\underset{\sim}{X}^{(0)}$. This procedure yielded excellent time histories for the state variables r, $\emptyset$, ρ, y and m. Utilizing Equation 1, and noting the impulses (velocity change) given by the two-impulse program, it was possible to accurately predict the duration of each "burn period". (Note that one first obtains the change in mass associated with the burn period, and that one must specify a set of rocket parameters; e.g. specific impulse, exhaust velocity, mass flow rate, etc.) In order to generate the initial conditions it was assumed that the impulsive take-off and arrival points occurred at the center of each burning period.

To avoid having a thrust initiation or termination point occur at $t = 0$ or $t = T$, a coasting arc of several hundred seconds duration

was assumed to occur at the beginning and end of the final optimal trajectory. Under this assumption it was a straightforward matter to compute exact initial and final values of the first four state variables. An initial approximation to the total time (T) required for the maneuver was obtained by summing the transfer times corresponding to the three impulsive coasting arcs.

Although the initial shape of the switching function (k) was unknown the impulsive solution gave an excellent approximation to the "switch points" (i.e., k = 0). In prior arguments it was established that only these critical values of the switching function are required for the generation of $\underset{\sim}{X}^{(k+1)}$. One may verify this by referring to Eqs. 53 to 58 and by noting that the Jacobian matrix contains no partial derivatives with respect to k except at a switching point. Note, however, that Eq. 53 also requires an initial guess as to the value of $\dot{k}$ at the switching points.

Having determined the time histories of the state variables and the switching times, it is also necessary to supply initial approximations to the time histories of the Lagrange multipliers. As previously noted, one of the Lagrange multipliers can be employed as a scale factor. Therefore, λ_1 was assigned an arbitrary initial value. The following relationship may then be constructed from Equation 31 by assuming that t = 0 at the impulsive switch point.(7)

$$\lambda_6 = \left(-\rho\lambda_1 - y\lambda_3\right) \Big/ \left(\frac{\dot{\rho}}{r \tan \nu} + \dot{y}\right) \qquad (59)$$

The impulsive solution may be employed to determine approximate values of r, ρ, y, $\dot{\rho}$, $\dot{y}$ and ν at the center of the initial burning period. By presuming an initial value for λ_3 one may then extract the resulting initial value for λ_6. An initial value for λ_4 then may be computed from the following expression which is a consequence of Equations 24 and 25:

$$\lambda_4 = \frac{\lambda_6}{r \tan \nu} \tag{60}$$

Thus, the initial values of the Lagrange multipliers can be established by utilizing the impulsive solution and guessing the ratio: λ_1/λ_3. Time histories of the Lagrange multipliers then were produced by an integration procedure which employed Equations 15 to 18 and utilized the previously stored impulsive time histories of the state variables. Figure 3 illustrates the validity of this procedure for a typical computer run by comparing the initial and converged time histories of several Lagrange multipliers. The initial approximations to the state variables were considerably better and, in most cases, differences between initial approximations and final converged values could not be detected when plotted to the scale of Figure 3. The fact that the state variables were initially well defined was important to achieving convergence of the quasilinearization technique.

VARIABLE LENGTH STORAGE TABLE

Although straightforward application of quasilinearization will result in a solution of the problems considered here, it was found necessary to employ a number of refinements to assure accuracy and proper convergence. For instance, when storing the tabular values of

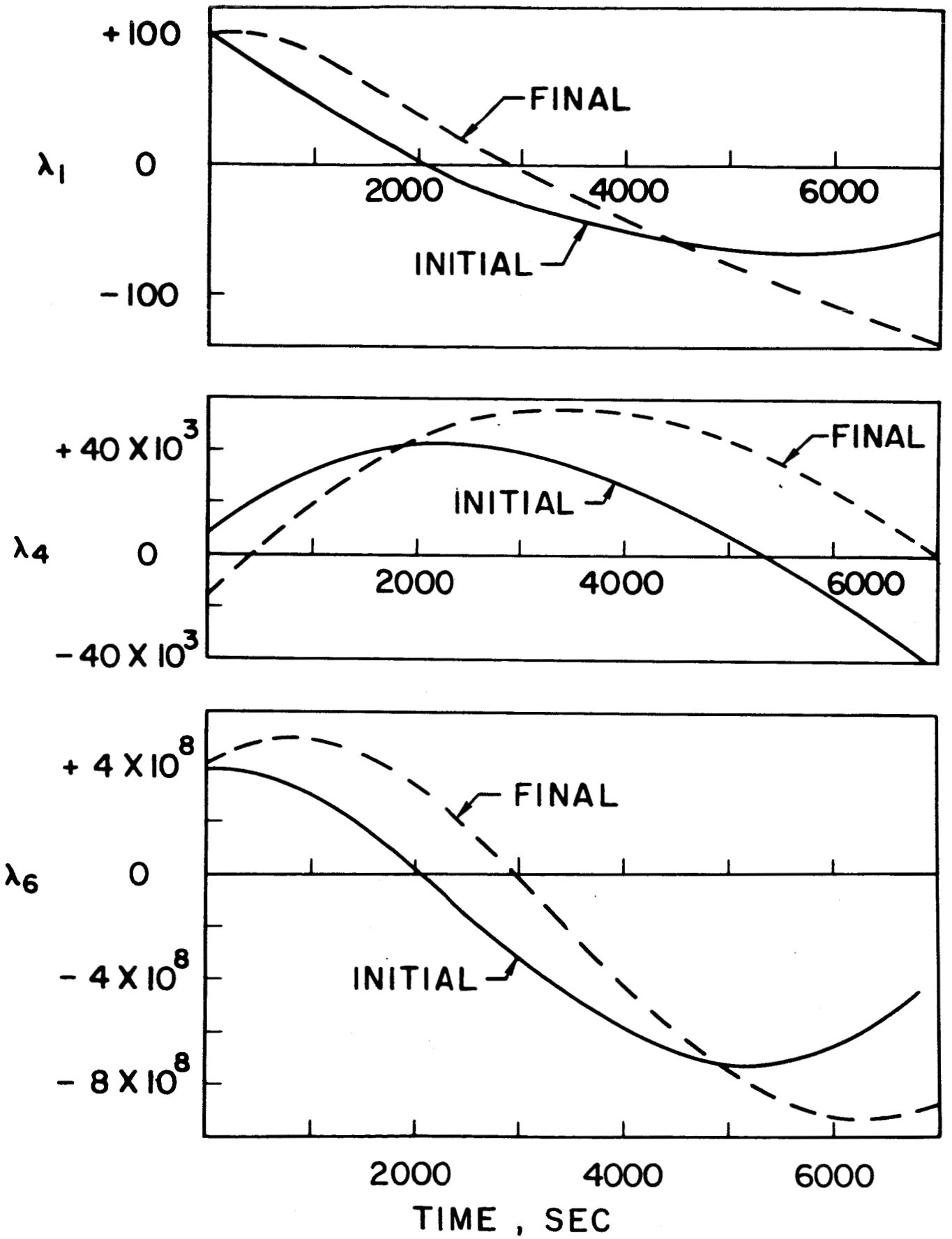

Figure 3 - Comparison of Initial and Converged Time Histories of Several Lagrange Multipliers

the solution $\underset{\sim}{X}^{(n)}$ for use in producing $\underset{\sim}{X}^{(n+1)}$ it was necessary to provide a method of maintaining integration accuracy over all portions of the trajectory. That is, it was found necessary to increase the data point storage density during the burning periods. For this reason, the quasilinearization process was constructed about a storage table having variable storage intervals. Figure 4a illustrates this concept. The basic quasilinearization subroutine described in Ref. 11 was programmed to integrate over each segment of the table and to stop at the boundaries. At this point a new storage interval would be introduced and the process continued.

SHIFTING STORAGE TABLE

Because the "bang-bang" control problem is inherently discontinuous at the corner points significant numerical problems are encountered. At such points one enters a new flight regime wherein $\dot{X}^{(n)}$ has entirely different properties. For this reason, the performance of valid numerical interpolation across a switching point is not normally possible.

As the quasilinearization process converges the switching times indicated by the n'th iteration will not coincide with those given by the n + 1'st iteration. If the switching point occurs between two table entries it is necessary to perform forward interpolation to arrive at appropriate stopping conditions and backward interpolation to arrive at appropriate numerical values to restart the integration. Since two different flight regimes are involved one finds that the interpolated values at the switching point, in general, do not agree. In many instances the above problem results in serious numerical errors or convergence failure.

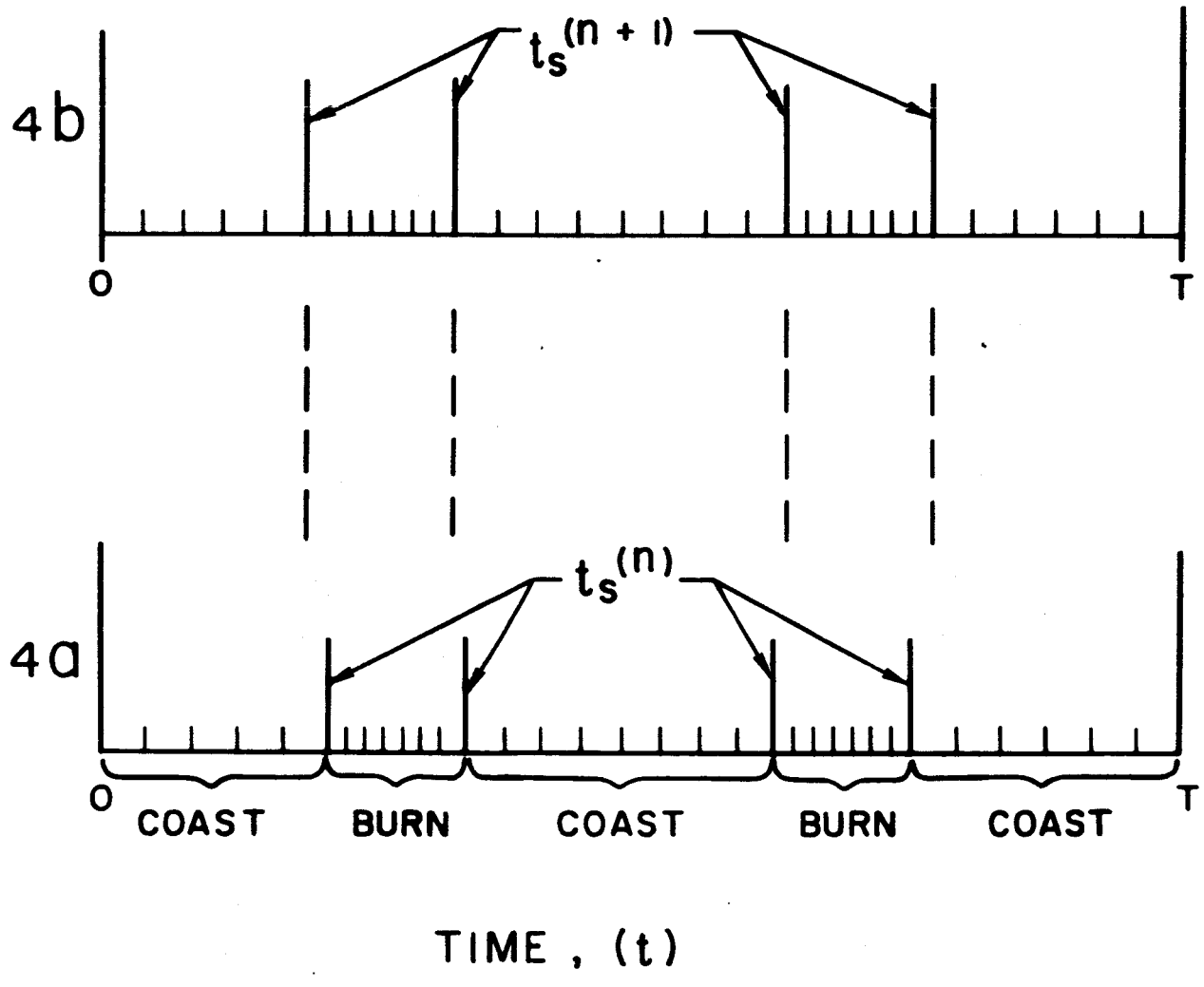

Figure 4 - Variable Length Storage Table (4a) and Table With Switching Points, t_s, Shifted for Next Iteration (4b)

One may employ another "trick" to insure numerical integration accuracy at the corner points. After each iteration of quasilinearization new switching times are determined which, in general, will not occur at the previous tabular values. A new table then may be constructed wherein the new switching times sre used to define the boundaries of each variable length storage array. This makes it possible to perform a new iteration of quasilinearization with the assurance that each stopping point coincides with a table entry. This new table and its relationship with that used in the prior iteration is illustrated in Figure 4b. Note that this method eliminates the necessity of interpolating to obtain the values at the stopping points. This numerical continuity across the corner points was found to be essential for the accurate convergence of the orbital transfers considered here.

SWITCH POINT ANALYSIS

As was pointed out earlier, the "bang-bang" control process produces trajectories which are very sensitive to the initiation, termination and duration of thrusting periods. It was therefore necessary to employ a rather sophisticated process for determining and controlling the switching times to be utilized in the determination of $\underset{\sim}{X}^{(n+1)}$.

A numerical procedure for determining the zeroes of the switching function was employed at the end of each quasilinearization iteration. If the new switching times showed large deviations from the previously used values, the new times would not be adopted. Instead, the program would shift the thrust initiation and termination times by a small portion of the indicated change.

Newly determined switching times would be fully utilized only when close agreement with the previous iteration had been achieved. In general, such close agreement could only be expected to occur after the quasilinearization process had proceeded through several iterations. However, once this requirement was met, the program was completely free to use the switching times indicated by the n'th iteration during the computation of the n + 1'st. The above programmed constraints forced the solution to conform to impulsive initial conditions until the process had achieved sufficient convergence to adequately control itself. Without this constraint and without the judicious use of the impulsive initial conditions it was usually impossible to obtain convergence.

V. NUMERICAL RESULTS

The forementioned IBM 7094 double precision program was utilized to generate transfers between arbitrary coplanar non-coapsidal orbits. Numerical results are best described by comparing the optimal finite thrust solutions with corresponding optimal impulsive transfers.

CONTROL VARIABLES

As was previously noted, the state variable time histories produced from the impulsive solution showed excellent agreement with the corresponding values for the finite thrust maneuver. Similar agreement was found for the control variables. This is best illustrated by an example. Initial, final and transfer orbits corresponding to an optimal finite-thrust transfer are depicted in Figure 5. The orbit and vehicle parameters are as follows: $p_1 = 5{,}000$ mi., $p_2 = 6{,}000$ mi., $e_1 = e_2 = 0.2$, $\omega_1 = -90°$, $\omega_2 = +30°$, $\beta = .0001$ m_o/sec. and initial $F/W = 0.4$. Figure 5 also indicates the directions and relative magnitudes of the two impulses ($\underline{F}_1$ and $\underline{F}_2$). The transfer orbit of the optimal finite thrust transfer coincides with its impulsive counterpart when plotted to the scale of Figure 5. The small arcs over which the engine is burning are also noted.

Figure 6 presents a time history of steering angle, ν, for the orbit transfer maneuver depicted in Figure 5. Note that only a small portion of the steering angle curve has physical significance. These two portions of the curve are expanded in the inset diagrams of Figure 6. The inset diagrams also give the impulsive steering angle for comparison

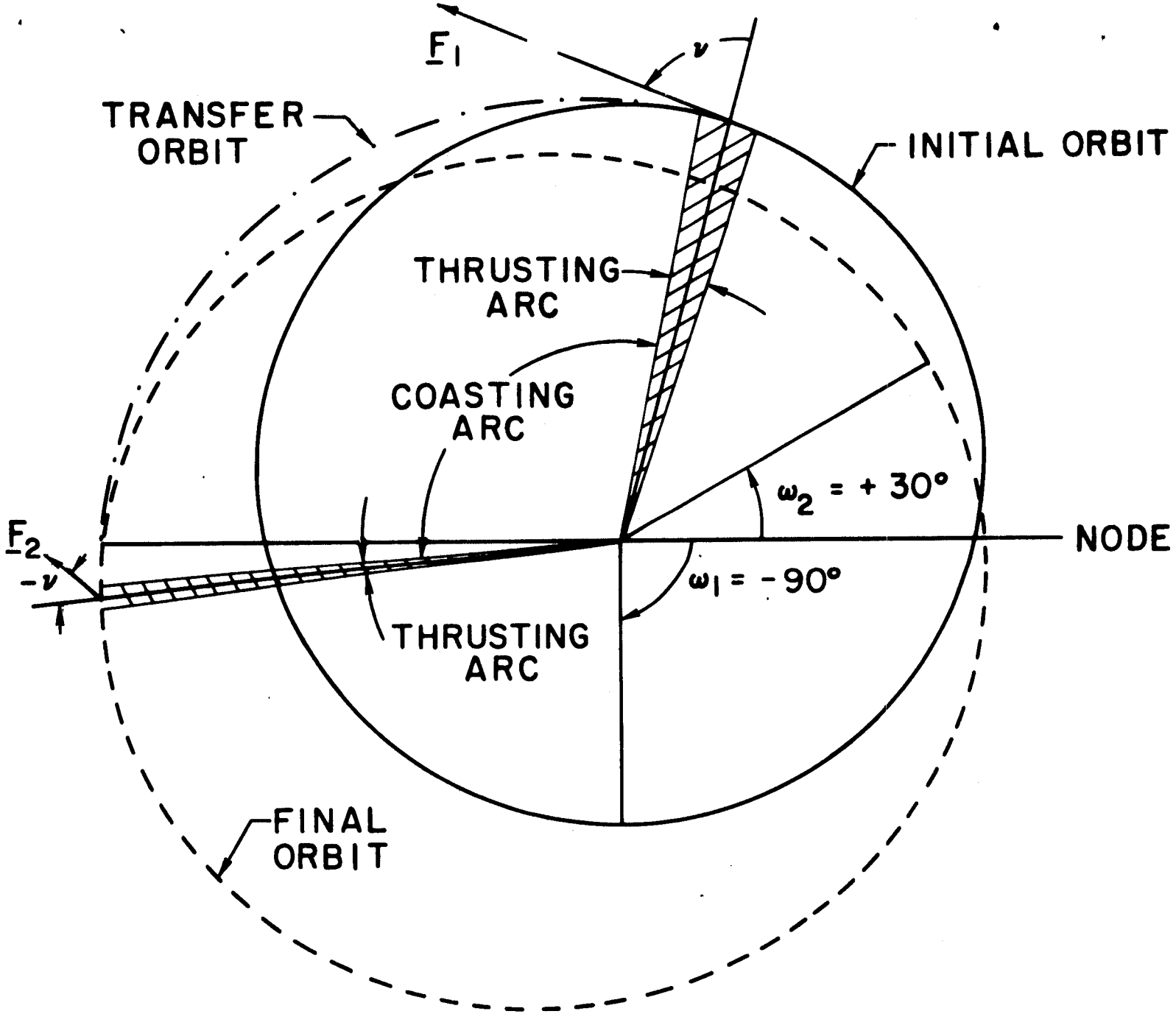

Figure 5 - Geometry of an Optimal Finite-Thrust Transfer Maneuver
(Thrust Vectors and Steering Angles for an Impulsive Transfer)

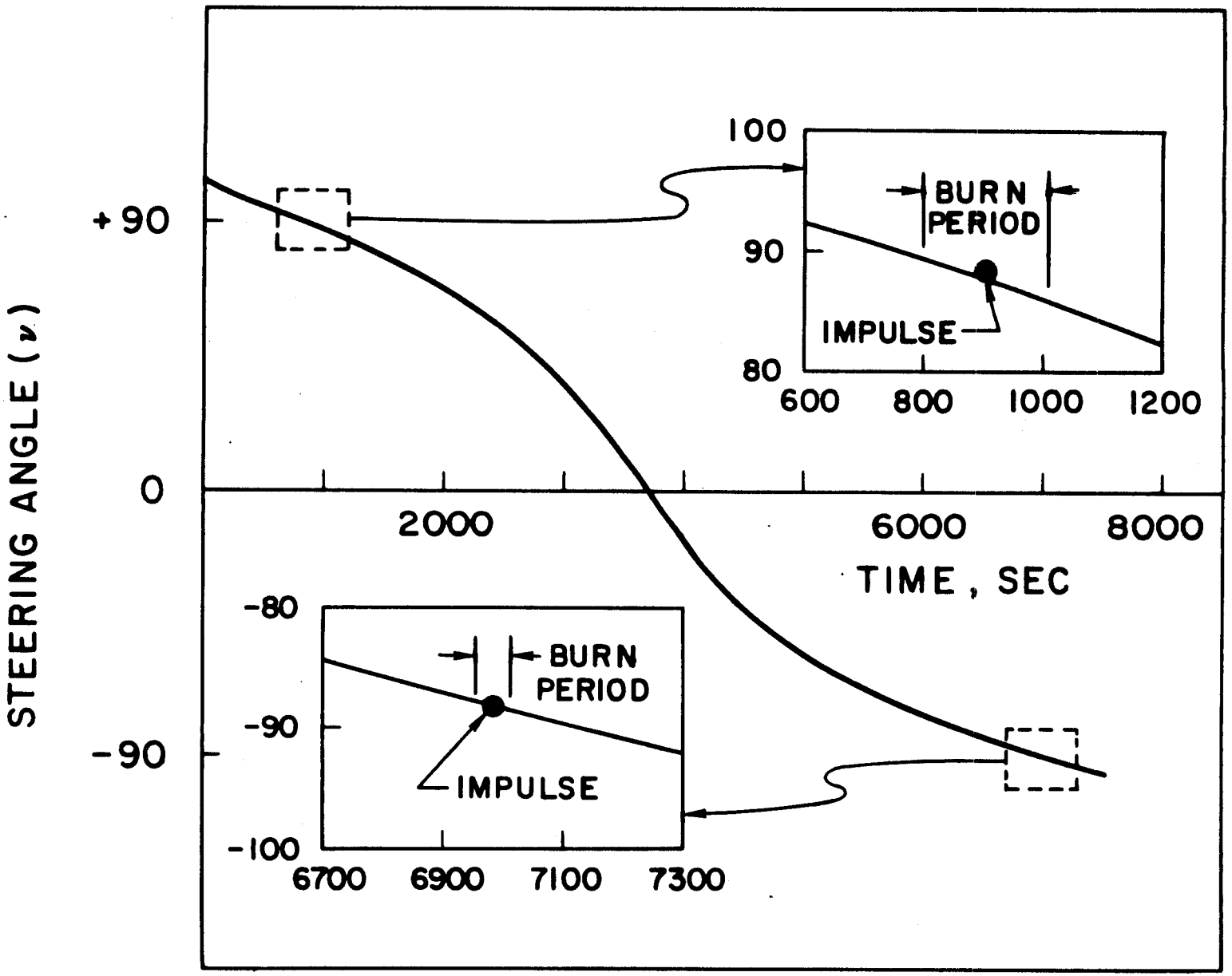

Figure 6 - Steering Angle History Compared to Corresponding Impulsive Thrust Angles

with the finite thrust solution. For this intermediate thrust case, the thrust initiation and termination times derived from the impulsive solution differed by only a few seconds from those indicated by the quasilinearization solution.

The switching function for this maneuver appears as Figure 7. It is clear that the engine is burning for a small portion of the total time required for the orbital transfer. In order to achieve adequate convergence of the quasilinearization process the switching times must be determined to approximately 0.001 seconds. Referring to Figure 7 and noting that the maneuver may involve several thousand seconds, one obtains an appreciation for the accuracy which must be maintained. Furthermore, when one considers that this accuracy must be maintained during the computations inherent in Equation 21, it is clear that double precision arithmetic is a necessity.

CONVERGENCE AND VALIDITY TESTS

Several tests of a solution's convergence and validity are available. First, because the best approximation to $\underset{\sim}{P}(0)$ is utilized for each iteration, the C_j appearing in Equation 40 should approach zero as the process converges. This provides the first test of convergence. Another test of convergence may be performed by noting successive values of the ξ_i given by Equation 42. During successive iterations the ξ_i should also approach zero. One should also observe the switching times approaching appropriate constant values during successive iterations. Also, since k must be zero at each switch point one should observe appropriate tabular values of k becoming successively smaller with each iteration. All of the above convergence criteria were achieved during the computation of the

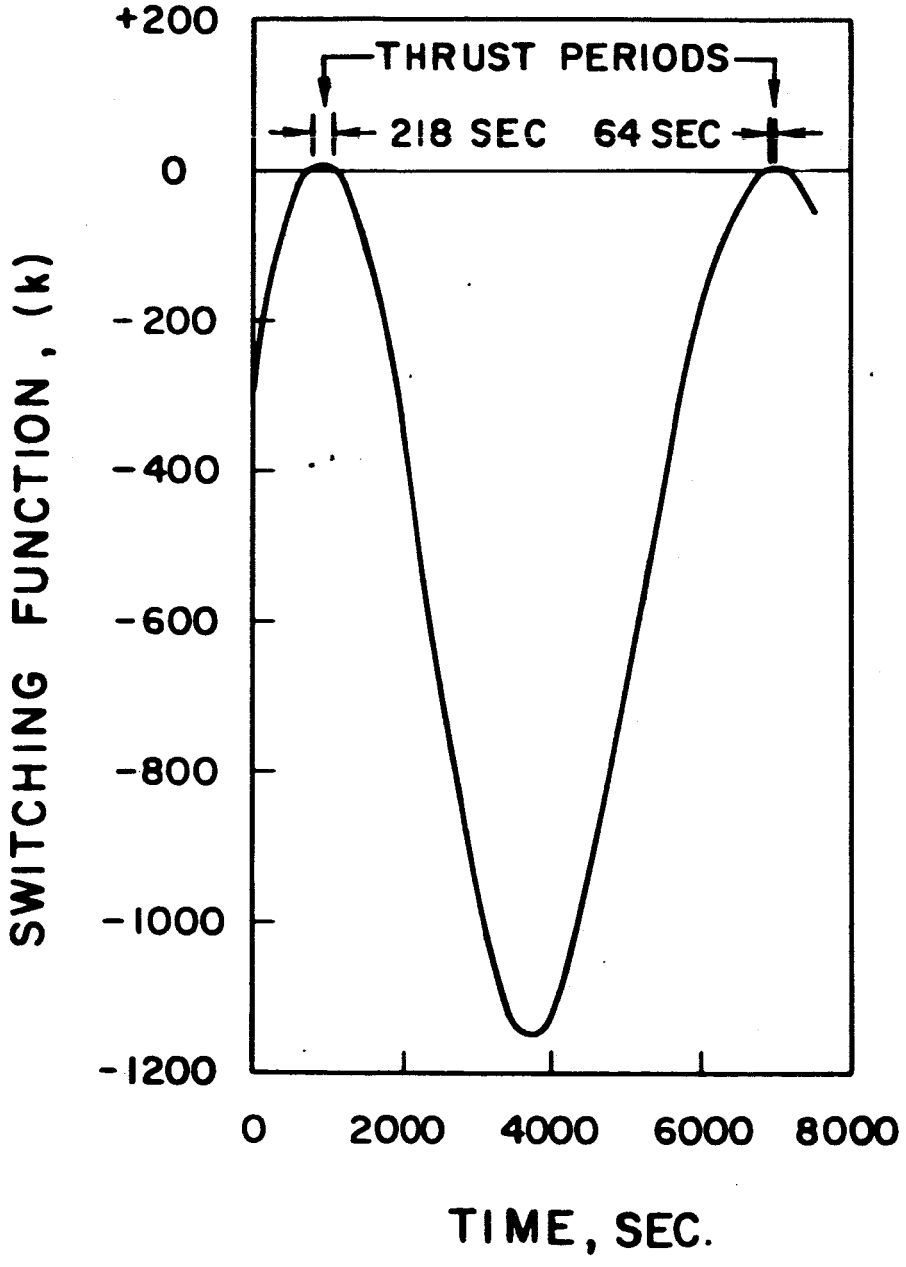

Figure 7 - Switching Function Time History

solutions presented here.

One may compute certain constants of motion as a test of the solution's validity, accuracy, etc. For instance, the Hamiltonian which is given by Equation 27 must remain constant. Of course, it is also possible to compute energy and angular momentum along the coasting arcs and note if these constants are really constant. For all of the results presented here, solutions wherein energy and angular momentum remained constant to more than eight significant figures were achieved. Similar accuracy was achieved for the Hamiltonian. Although this extreme accuracy would not ordinarily be necessary for engineering studies, it was required for the accurate comparison of finite thrust maneuvers and their impulsive counterparts.

As a final test, the converged solution $X^{(\infty)}(0)$, was utilized as initial conditions for a straightforward integration of the Euler Lagrange differential equations. The solution produced by this method was then compared with that generated by quasilinearization. In all cases this test confirmed the validity of the quasilinearization solution.

MINIMUM FUEL WITH FINAL TIME OPEN

Because the transfer time (T) derived from the impulsive solution is slightly nonoptimal additional computations must be performed to determine that trajectory which is time-optimal as well as fuel-optimal. Since the Hamiltonian may be thought of as the partial derivative of final mass with respect to T it is necessary to adjust T until the Hamiltonian approaches zero. This was accomplished by perturbing T and computing an additional fuel-optimal trajectory. This required several additional quasilinearization iterations. The Hamiltonian corresponding to each of the fuel-

optimal trajectories was examined and simple linear extrapolation was used to predict a new value of T corresponding to A = 0. Thus, it was possible to compute a trajectory for which T was "locally" optimal.

ΔV REQUIREMENTS (IMPULSIVE THRUST vs. FINITE THRUST)

Numerous optimal trajectories were computed in order to produce a comparison of optimal impulsive transfers and corresponding finite-thrust maneuvers. Figure 8 compares the velocity change (ΔV) required for finite-thrust and two-impulse maneuvers over a wide range of initial thrust-to-weight ratios (F/W). It was produced by beginning with the transfer maneuver depicted in Figure 6 and parametrically varying the specific impulse (note that β was held constant). The original log-log plot of this data showed no deviation from a straight line (parabola) over the range shown. The fact that the impulsive orbital transfer is a very close approximation to the finite thrust maneuver is verified by the small percentage differences in Figure 8.

Another interesting comparison was produced by varying the relative perigee angle ($\Delta\omega$) of the two coplanar elliptical orbits of Figure 6. Figure 9 demonstrates that the difference in velocity change required for impulsive and the finite thrust maneuvers exhibits a strong dependence upon $\Delta\omega$. The curve is divided into two regimes corresponding to intersecting and non-intersecting orbits. Near the value of $\Delta\omega$ which corresponds to tangency ($\Delta\omega = 53°.1301$) the curve abruptly, but continuously, changes.

This particular phenomenon is best explained by reference to Figure 10 which contains curves for the two-impulse and finite thrust maneuvers as separate plots. Figure 10 concerns a small range of $\Delta\omega$ over which the orbits are "almost tangent". Since it was known that the class of "almost

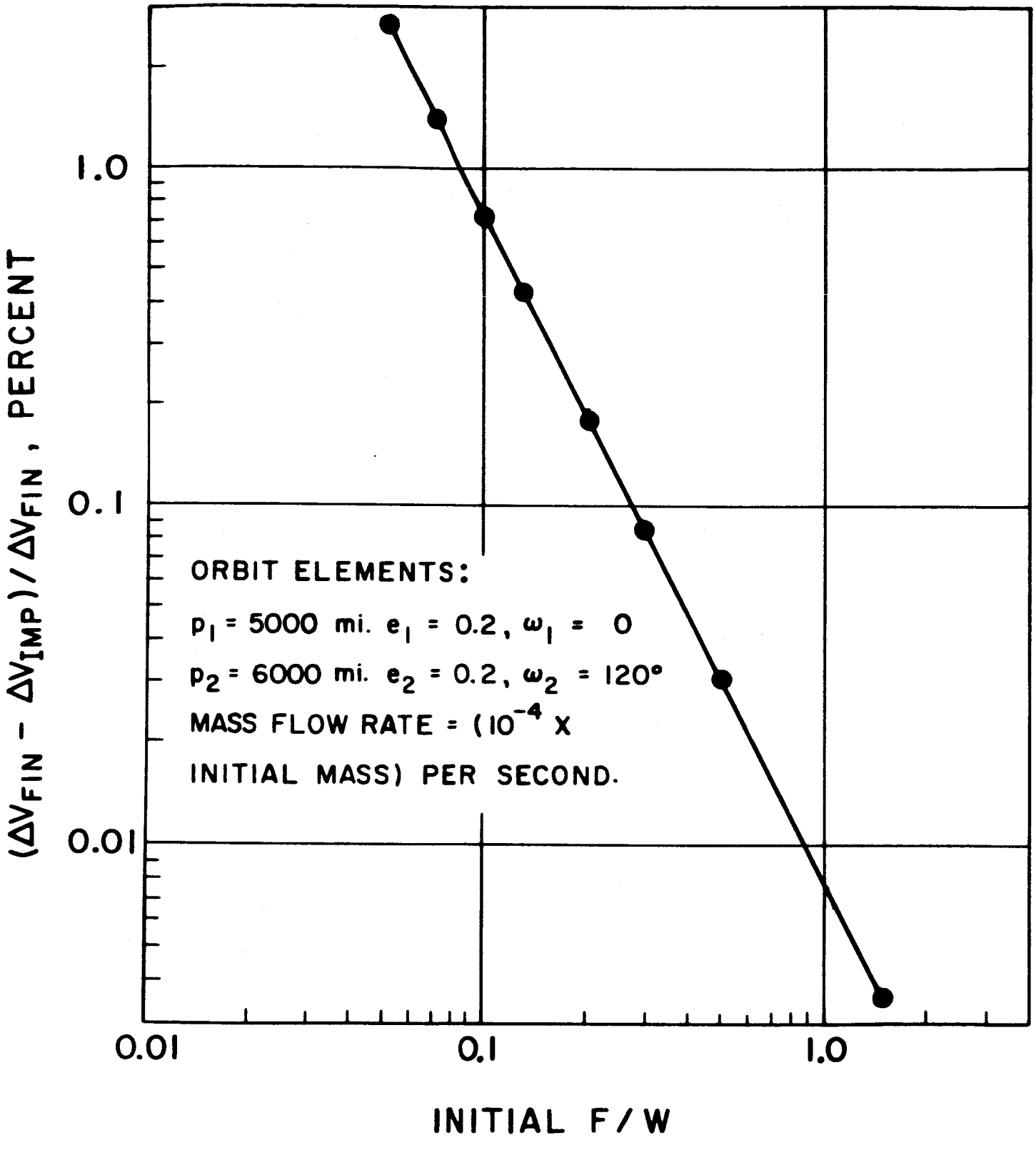

Figure 8 - Difference in ΔV Required for Finite-Thrust and Impulsive Transfers versus Initial Thrust-To-Weight Ratio

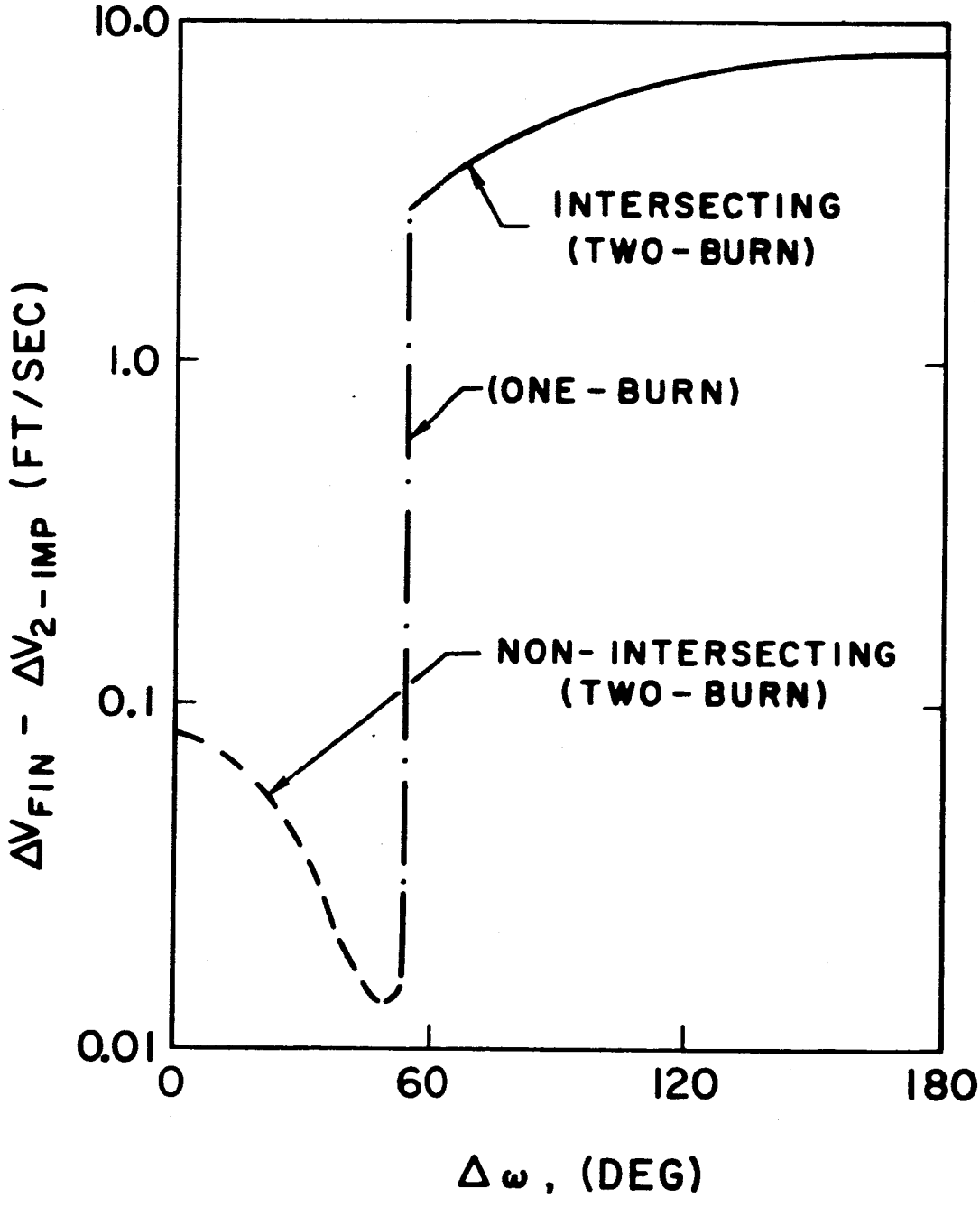

Figure 9 - ΔV Difference as a Function of the Relative Perigee Orientation of Two Elliptical Orbits

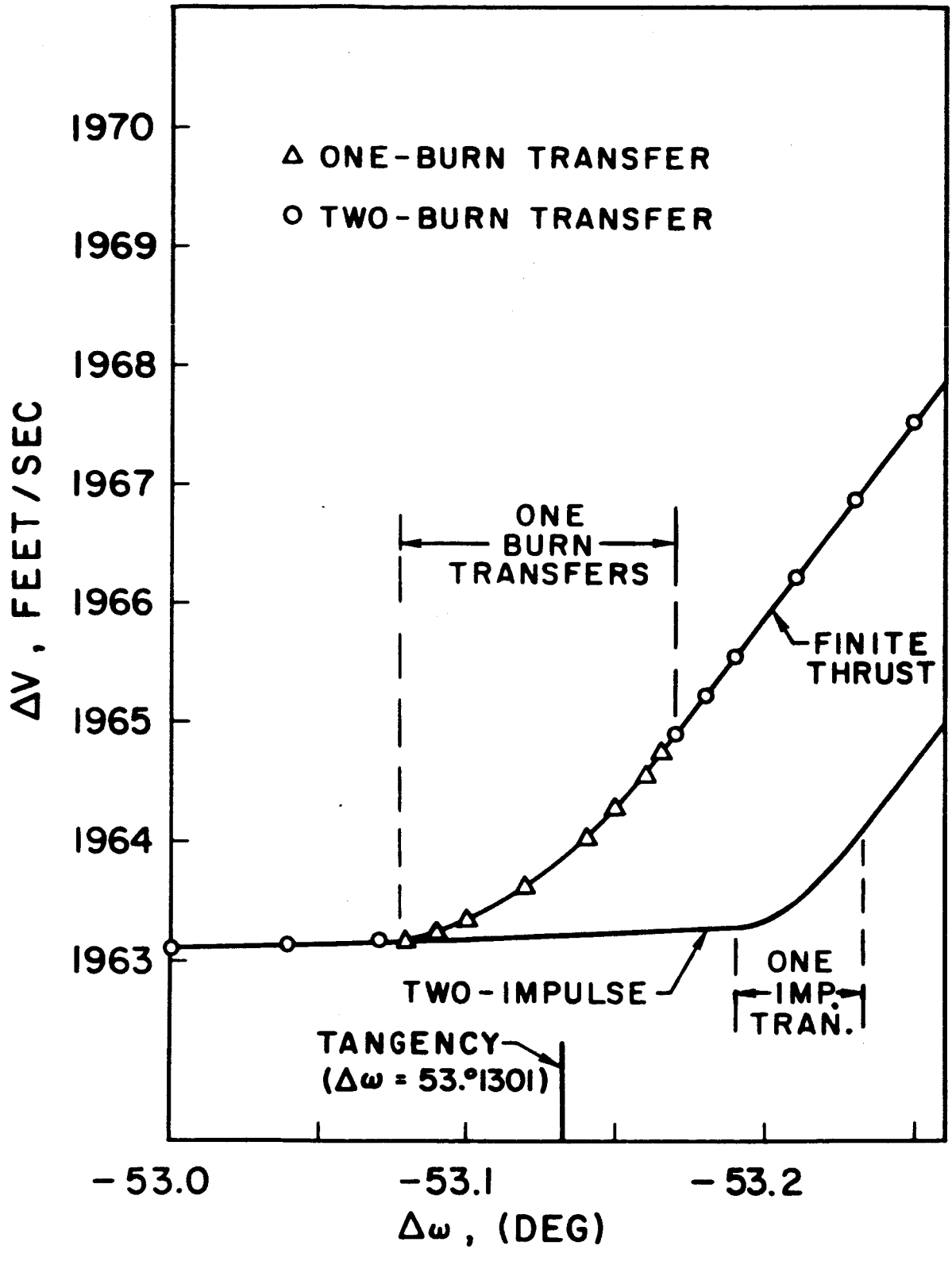

Figure 10 - Velocity Change Required for Finite-Thrust and Impulsive Transfers Between "Almost Tangent" Orbits

tangent" orbits produced a number of interesting results (Refs. 7 and 8) considerable effort was devoted to accuracy in examining these critical orientations. Note that the two curves are nearly coincident as long as the orbits do not intersect and that the curves become separate as intersection deepens. This sudden diverging of the two curves in Figure 10 explains the abrupt change noted in Figure 9. The magnitude of this difference depends upon the particular rocket parameters employed (e.g., specific impulses, mass flow rate, etc.).

In Refs. 14, 15 and 16 the existence of an optimal one-impulse maneuver was discussed. The two-impulse curve shown in Figure 10 contains a small region over which a one-impulse transfer between the two orbits is optimal. The finite thrust curve is composed of a number of points which are designated one burn maneuvers or two burn maneuvers. Note that an optimal one burn maneuver also exists over a small range of $\Delta\omega$. Thus, one obtains conditions which are again analogous to those found for impulsive transfer.

As in the impulsive case, the maneuvers represented by points directly on either side of the one burn region are characterized by entirely different steering angle, and thrust time histories. To the left of the one-burn region the first burn period is rather small and the thrust for both burns is in the forward direction. To the right of the one-burn region the second burn period is very small and its thrust direction opposes the vehicle's velocity vector. Figure 11 presents the switching function time histories associated with each of three kinds of finite thrust maneuvers considered in Figure 10. For the two burn transfers the duration of the smaller burn periods was a fraction of a

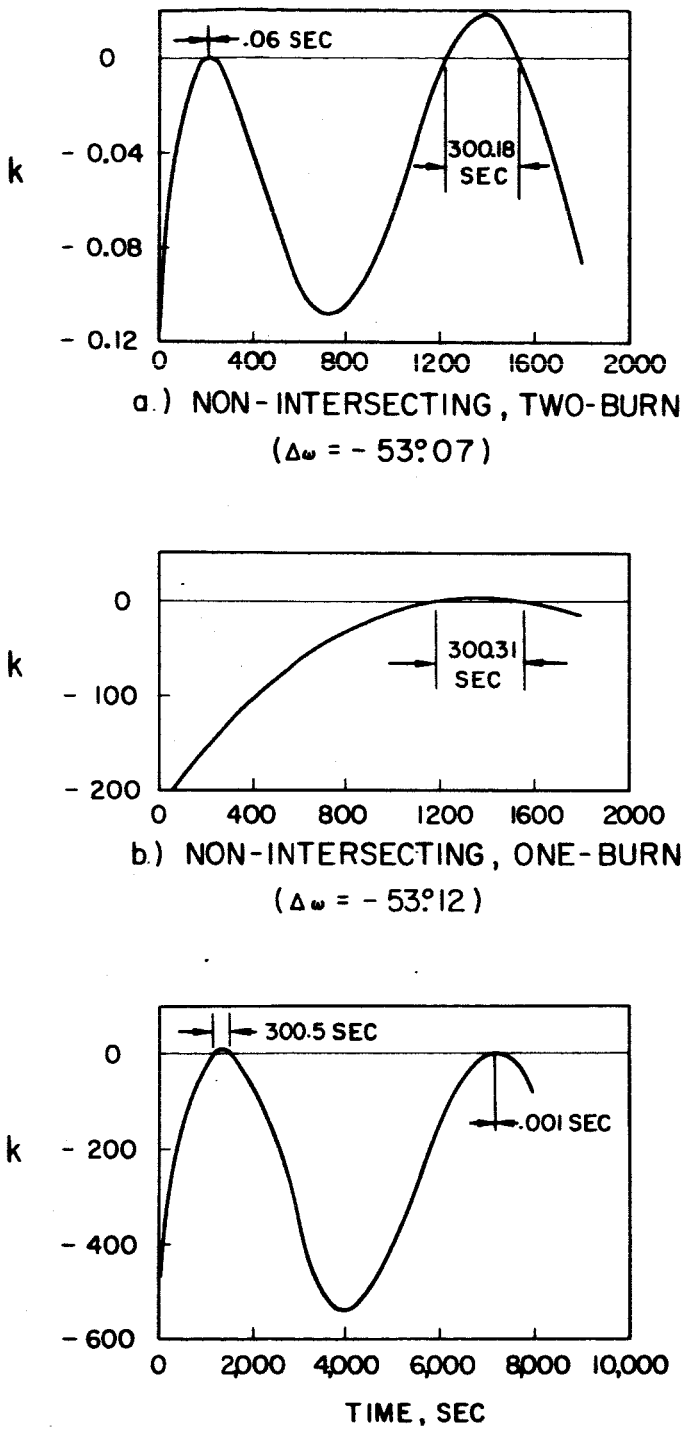

Figure 11 - Switching Function Time Histories for Several Transfers Between "Almost Tangent" Orbits

second as compared to about 300 seconds for the larger burn period. Some solutions which were near the boundary of the one-burn region exhibited a second burn period of .002 seconds duration and smaller. The extreme numerical accuracy required to produce the results of Figure 9 and 10 should be evident.

VI. CONCLUSION

The numerical results demonstrate that the quasilinearization technique can be a powerful tool for the optimization of "bang-bang" control problems. However, it appears that a good first approximation to the solution is required to insure convergence. In general, it appears that impulsive orbital transfer maneuvers provide an excellent approximation to their finite thrust counterparts. For this reason most preliminary engineering design studies could be performed with simple economical impulsive transfer optimization procedures, thus avoiding a more time consuming and difficult finite-thrust optimization.

VII. REFERENCES

1. Jurovics, Stephen A., "Orbital Transfer by Optimum Thrust Direction and Duration," North American Aviation, Inc., SID 64-29 (12 February 1964).
2. Kalaba, R., Some Aspects of Quasilinearization, (Nonlinear Differential Equations and Nonlinear Mechanics) New York; Academic Press, Inc., pp. 135-146 (1963).
3. Bellman, R., Kagiwada, H., and Kalaba, R., "Quasilinearization, System Identification and Prediction," RAND CORP., RM - 3812 PR (August 1963).
4. McGill, R. and Kenneth, P., "Solution of Variational Problems by Means of a Generalized Newton-Raphson Operator," AIAA J., 2, pp. 1761-1766 (October 1964).
5. McCue, G.A., "Optimum Two-Impulse Orbital Transfer and Rendezvous Between Inclined Elliptical Orbits," AIAA J., 1, pp. 1865-1872 (1963).
6. McCue, G.A., "Optimization and Visualization of Functions," AIAA J., 2, pp. 99-100 (January 1964).
7. McCue, G.A., and Bender, D.F., "Optimum Transfers Between Nearly Tangent Orbits," North American Aviation, Inc., SID 64-1097 (May 1, 1965).
8. McCue, G.A., and Bender, D.F., "Numerical Investigation of Minimum Impulse Orbital Transfer," AIAA J., 3, pp. 2328-2334 (December 1965).
9. Leitman, G., "Variational Problems With Bounded Control Variables," Optimization Techniques, edited by G. Leitman (Academic Press, New York) pp. 171-204 (1962).

10. Friedman, B., "Principles and Techniques of Applied Mathematics," John Wiley & Sons, Inc. (November 1962).

11. Radbill, J.R., and McCue, G.A., "QASLIN—A General Purpose Quasilinearization Program," North American Aviation, Inc., SID 66-394 (June 1, 1966).

12. Hildebrand, F.B., "Methods of Applied Mathematics," (Englewood Cliffs, New Jersey: Prentice-Hall, Inc.) pp. 34-35 (1952).

13. McCue, G.A. and Hoy, R.C., "Optimum Two-Impulse Orbital Transfer Program," North American Aviation, Inc., SID 65-1119 (August 1, 1965).

14. Contensou, P., "Etude theorique des trajectories optimales dans un champ de gravitation. Application au cas d'un center d'attraction unique," Astronaut. Acta 8, 134-150 (1963); also Grumman Research Dept. Translation TR-22 translated by P. Kenneth (August 1962).

15. Lawden, D.F., "Optimal Trajectories for Space Navigation," Butterworths Scientific Publications Ltd.,(London, 1963).

16. Breakwell, J.V., "Minimum Impulse Transfer," AIAA Preprint 63-416 (1963).

APPENDIX B*

TWO-IMPULSE TRANSFER IN THE THREE-BODY PROBLEM

*Note that this appendix is a separate paper having its own nomenclature, illustrations, references, etc.

CONTENTS

NOMENCLATURE

A_1, A_2	Angles of Perigee and Perilune (Figure 4)
c_1, c_2, c_3	Combination Coefficients of Homogeneous Solution Vectors
D	Earth-Moon Distance (Semi-Major Axis)
g_i, g	General Symbol for Expression for Time Derivative of X_j, Column Vector
G	Universal Constant of Gravitation Times Mass of Earth plus Moon
H	Homogeneous Solution Vector (of Equation 19)
i,j,k	Unit Vectors Along x,y,z
I	Impulse
J	Jacobian Matrix $\left(\frac{\partial g_i}{\partial X_j}\right)$
K	Jacobi Integral
P	Particular Solution Vector (of Equation 13)
r	Distance to Earth
s	Distance to Moon
t	Time (Independent Variable)
T	Time of Travel on Transfer Trajectory
u,v,w,V	Velocity Vector Components and Magnitude
x,y,z	Position Vector Components
X_j, X	General Symbol for Dependent Variable, Column Vector of Dependent Variables
ρ	Convergence Values for X, a Column Vector
ξ	$\underset{T}{\text{MAX}} \left\lvert X^{(n)}(t) - X^{(n+1)}(t) \right\rvert$, a Column Vector
μ	The Ratio Mass Moon to Mass Earth plus Moon

ω	Angular Velocity of the Moon in its Orbit

Subscripts

o	For Departure Point at t = 0
T	For Arrival Point at t = T
t	For Transfer Trajectory

Superscript represents the iteration number, e.g. $X^{(n)}$

Underline signifies a vector in three dimensions.

ILLUSTRATIONS

ABSTRACT

A computer program for finding two-impulse transfers between given terminal points in a fixed time in the three-body problem has been developed. The only restriction is that the third body, which is imagined to be a space ship, exerts a negligible attraction on the two large centers. It generates a patched conic to use as an initial trajectory and uses the quasilinearization process to correct the trajectory so that the two-point boundary value problem is solved. The program and its use are described in detail and preliminary results showing excellent convergence properties are presented.

I. INTRODUCTION

Suppose it is desired that a spaceship on some orbit in Earth-Moon space transfer to a new orbit by means of a two-impulse maneuver. While this problem is topologically similar to two-impulse transfer in the two-body problem there are two significant differences from the computational and analytic points of view. In the first place the orbits are not generally cyclic and points along them cannot be represented by five orbital elements and an angle. The six components of position and velocity are used instead. The second major difference is that the given information concerning the departure and arrival points does not permit one to describe transfer orbits as a known function of any one parameter. In general there is a single infinity of orbits through two given points and in the two-body case one can choose, for example, the semi-latus rectum of the transfer orbit as the parameter. It is then possible to immediately compute the orbit, the velocities at both ends, and the impulses. In the three-body case the author chose to span the infinity of orbits by using time to transfer as the parameter. To obtain the orbit, the velocities at both ends, and the impulses, is a major problem. It was the aim of this portion of the work to provide a computer program to compute these quantities. That is, from the given departure point (B_o in Figure 1), the given arrival point (B_T in Figure 1), and the given time interval (T), the program is to determine the transfer orbit trajectory, the velocities at both ends, and the impulses. It was possible to accomplish this for

the reduced three-body problem in which the third body does not affect the motion of the two primary bodies. The two large bodies may move in either circular or elliptical orbits about their center of mass.

This program represents the first necessary step in a longer range problem which is the numerical analysis of two-impulse transfers in Earth-Moon space. Now that it has been developed a systematic study of two-impulse transfers can be undertaken.

II. PROBLEM FORMULATION

The computational problem involved is a highly non-linear two-point boundary value problem and the method of solution utilizes a generalized Newton-Raphson[1] technique which is called quasilinearization.

In the complete program as it is described below the input and output coordinate systems may be centered at the Earth, the Moon, or their barycenter and the systems may be rotating or inertial. However, the computations are all managed in the rotating system centered at the barycenter and the problem will be described in this system. The equations of motion are easily derived using the Lagrangian procedure. Extra terms involving $\dot{\omega}$ occur since the rotating system usually does not rotate uniformly. We find:

$$\dot{u} = 2\omega v + \omega^2 x - \frac{\mu G(x-(1-\mu)D)}{s^3} - \frac{(1-\mu)G(x+D)}{r^3} + \dot{\omega} y \tag{1}$$

$$\dot{v} = -2\omega u + \omega^2 y - \frac{\mu G y}{s^3} - \frac{(1-\mu)Gy}{r^3} - \dot{\omega} x \tag{2}$$

$$\dot{w} = \frac{-\mu G z}{s^3} - \frac{(1-\mu)Gz}{r^3} \tag{3}$$

$$\dot{x} = u \tag{4}$$

$$\dot{y} = v \tag{5}$$

$$\dot{z} = w \tag{6}$$

As shown in Figure 1 the xy plane is the plane of the Earth-Moon motion and the x axis is directed toward the instantaneous position of the moon. G is the universal gravitational constant times the total mass of the

Earth-Moon system, μ equals the mass of the moon divided by the total mass of the system, D is the Earth-Moon distance (or a semi-major axis of the orbit if it is elliptical), and ω is the angular velocity of the system. For the restricted problem in which the two primaries are assumed to be in circular orbits the equations simplify somewhat since $\dot{\omega} = 0$ and they possess a well known integral, the Jacobi integral, which is

$$K = -V^2 + \frac{2(1-\mu)G}{r} + \frac{2\mu G}{s} + \omega^2 (x^2 + y^2) \qquad (7)$$

Two different unit systems are provided for in the program. One is based on the metric system using kilometers for distance and seconds for time. The second system uses lunar units for which $\omega = 1$ rad per unit time, D = 1 lunar distance, and $G = 1\ (l.d.)^3/(U.T.)^2$

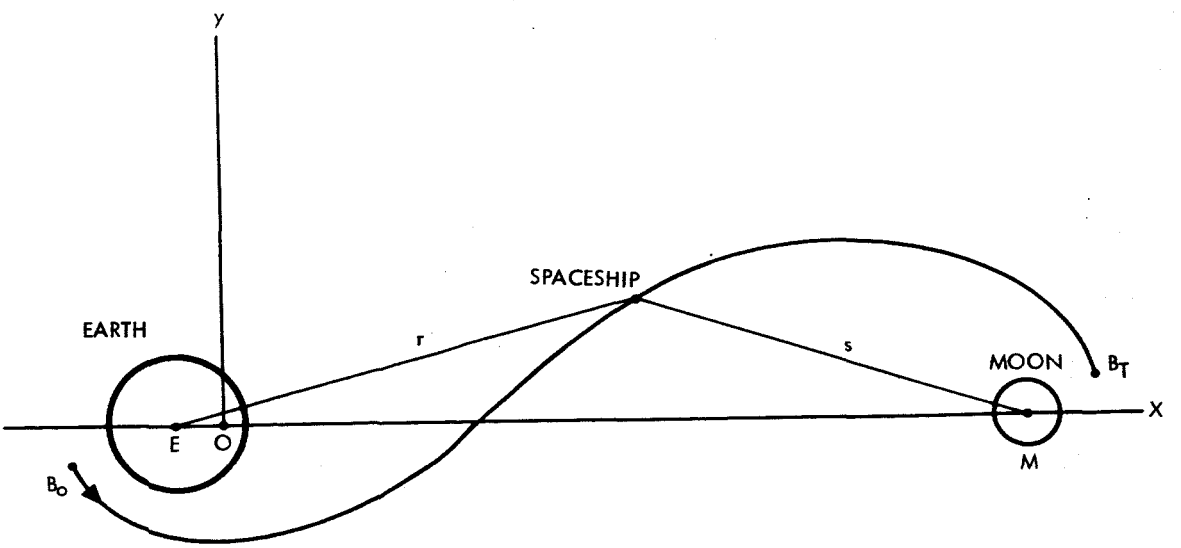

B_O = DEPARTURE $(u_O, v_O, w_O, x_O, y_O, z_O)$ EM = D

B_T = ARRIVAL $(u_T, v_T, w_T, x_T, y_T, z_T)$ EO = μ D

Figure 1. The Rotating Coordinate System

The problem is described as follows. Given the initial position (x_o,y_o,z_o), the final position (x_T,y_T,z_T), the time (T), and the general shape of the desired transfer trajectory, we wish to find the trajectory and the velocities at t = 0 and t = T. That is,we wish to find the velocity (u_{to},v_{to},w_{to}) at t = 0 which will cause the vehicle to arrive at (x_T,y_T,z_T) at the time T later. The solution is to be accomplished using the quasilinearization procedure which is described in Appendix A Section III, and in Ref. 1. It is seen that this set of equations (Eqs. 1 to 6) is of the form of Equation 35 (App.A), and that the feasibility of using the procedure depends upon finding analytic expressions for the derivatives of the right hand sides (g_i) with respect to the six variables (X_j), i.e., upon obtaining the Jacobian matrix, J. This is easily accomplished and the matrix for the general three-body trajectory is given in Equation 8.

$$J=\left(J_{ij}\right)=\left(\frac{\partial gi}{\partial X_j}\right)=\begin{bmatrix} 0 & 2\omega & 0 & \omega^2-A+E & \dot{\omega}+By & Bz \\ -2\omega & 0 & 0 & -\dot{\omega}+By & \left(\omega^2-A+Cy^2\right) & Cyz \\ 0 & 0 & 0 & Bz & Cyz & -A+Cz^2 \\ 1 & 0 & 0 & 0 & 0 & 0 \\ 0 & 1 & 0 & 0 & 0 & 0 \\ 0 & 0 & 1 & 0 & 0 & 0 \end{bmatrix} \tag{8}$$

where

$$A = \left[\frac{1-\mu}{r^3} + \frac{\mu}{s^3}\right] G \tag{9}$$

$$B = \frac{3(1-\mu)G}{r^5}(x + \mu D) + \frac{3\mu G(x-(1-\mu)D)}{s^5} \tag{10}$$

$$C = \frac{3(1-\mu)G}{r^5} + \frac{3\mu G}{s^5} \tag{11}$$

$$E = + \frac{3(1-\mu)G(x+ D)^2}{r^5} + \frac{3\mu}{s^5} G (x-(1-\mu)D)^2 \tag{12}$$

The (n+1)'th iteration $X^{(n+1)}$, is obtained as follows from the n'th iteration, $X^{(n)}$, and the approximate differential equation (Eq. 37, App. A in matrix form):

$$\dot{X}^{(n+1)} = g(X^{(n)}) + J(X^{(n)}) \cdot (X^{(n+1)} - X^{(n)}) \tag{13}$$

A particular integral, P, is obtained from the previous time history by integrating Equation 13 starting with the initial values from the last iteration $(u_o^{(n)}, v_o^{(n)}, w_o^{(n)}, x_o, y_o, z_o)$*. At the same time a set of three homogeneous solutions to

$$\dot{H} = J(X^{(n)})\, H \tag{14}$$

are generated with initial conditions $(V_1,0,0,0,0,0)$*, $(0,V_2,0,0,0,0)$*, and $(0,0,V_3,0,0,0)$*. The linearity of Equation 7 in $X^{(n+1)}$ allows the new iteration, Equation 10, to be P plus a linear combination of the three solutions.

$$X^{(n+1)} = P + c_1H_1 + c_2H_2 + c_3H_3 \tag{15}$$

The coefficients (c_1,c_2,c_3) are determined by requiring the solution to satisfy the boundary conditions at the final position (x_T,y_T,z_T).

*The vectors X,g,H and ξ are really column vectors but the initial values are printed here as rows for convenience in typing.

As explained in Appendix A (p. 13) convergence of the process is examined by evaluating the maximum change (at any point) between successive iterations in each coordinate (Equation 42, App. A).

$$\xi = \underset{T}{MAX} \left| X^{(n)}(t) - X^{(n+1)}(t) \right| \tag{16}$$

Only when every component of ξ has satisfied given conditions is the procedure declared to have converged.

At the end of each iteration the impulses are computed at the beginning and at the end of the trajectory. We use

$$\underline{I}_1 = (u_o^{(n)} - u_o)\underline{i} + (v_o^{(n)} - v_o)\underline{j} + (w_o^{(n)} - w_o)\,\underline{k} \tag{17}$$

$$\underline{I}_T = (u_T^{(n)} - u_T)\underline{i} + (v_T^{(n)} - v)\underline{j} + (w_T^{(n)} - w_o)\,\underline{k} \tag{18}$$

$$I = I_o + I_T = \sqrt{I_o \cdot I_o} + \sqrt{I_T \cdot I_T} \tag{19}$$

If the process converges within the assigned limit of iterations the program transfers to a mode in which the actual equations are integrated with the complete set of initial conditions as determined by QASLIN. The vector, ξ, now gives the differences between the final iteration and this integral and it will indicate how well this final integral represents the solution to the desired problem since the differences between the coordinates of the final point reached and those of the given end point are included in the comparison.

III. COMPUTER PROGRAM DESCRIPTION

A computer program written in double precision FORTRAN IV language has been developed for solving the problem of finding two-impulse transfers between given points in Earth-Moon space. It was developed to provide wide capability and has the following set of general properties:

a. The initial and final conditions can be given in any two of a series of coordinate systems centered at the Earth or the Moon or the barycenter. Orbital elements for close Earth orbits and/or close Moon orbits are permissible.

b. Two unit systems are presently available: metric with kilometers and seconds or lunar units with $\omega = D = G = 1$ (see Equation 1-6 above). The total trip time, however, must be given in hours. Provision for a third system exists in the program. The actual constants used are provided in a single short subroutine and can easily be changed.

c. Real time with the initial epoch in modified Julian Days may be used and the Moon's position will be determined by the program. The secular motion of the lunar orbit node and perigee during the trip time are neglected. Or, an artificial reference time may be used with the moon's initial position anywhere in its orbit.

d. The orbits of the Earth and Moon may be assumed to be circular or elliptical.

A block diagram of the overall computer program is shown in Figure 2. The general operation of the program is clear from this diagram and the details of using the program are described below under the following

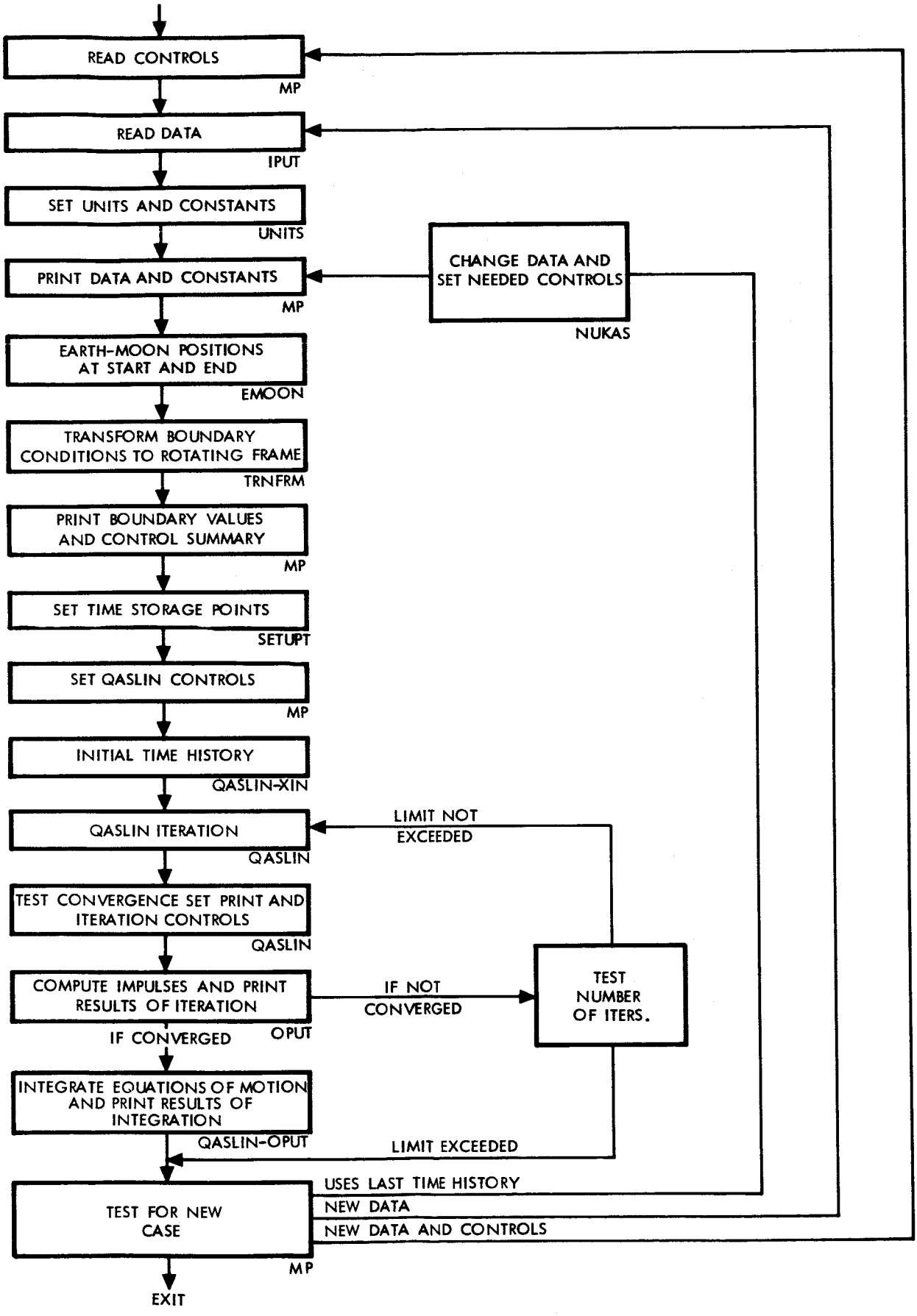

Figure 2 - Flow Diagram For Two-Impulse Computation

headings:

1. Input Data Coordinate Systems
2. Constants
3. Data Entry
4. Program Controls
5. Time History Storage
6. Initial Time History
7. Subroutine QASLIN
8. Program Output

This program has been designed with a great flexibility for input conditions. Unfortunately, at this moment the program is so close to exceeding the allowable storage on the IBM 7094 that it has been found necessary to make use of two slightly different versions. These are obtained by using dummy subroutines when a job is being sent which does not use a particular section. Since the portion of the program for the computations of the initial time history is used only once for a given case and is independent of the later iteration process it is believed that an overlay process can be developed which will require very little extra computer time. This would allow a further increase in the total number of time storage points if accuracy requirements should demand an increase.

1. Input Data Coordinate Systems

As already mentioned, the initial and final boundary conditions may be given in Earth centered, Moon centered, or barycentric systems. These are specified by the values ICORC(I) = J where: I = 1, 2 for initial, final conditions; and J = 1, 2, 3 for Earth, Moon, barycenter. A second integer IROTS(I) further identifies the systems according to the scheme shown in Table 1.

TABLE 1. COORDINATE SYSTEM FOR INPUT BOUNDARY CONDITIONS

	ICORC(I) = / IROTS(I) =		J=1 Earth Centered	J=2 Moon Centered	J=3 Barycenter Centered
Cartesian boundary conditions	Rotating System	1	x axis toward moon - xy plane is LOP	x axis opposite earth xy plane is LOP	x axis toward moon xy plane is LOP
	non rotating system	2	x axis toward moon's orbit node on ecliptic xy plane is LOP	x axis toward moon's orbit node on lunar equator xy plane is LOP	x axis toward moon's orbit node on ecliptic
		3	x axis toward vernal equinox xy plane is ecliptic	x axis toward node xy plane is lunar equator	not used
		4	x axis toward vernal equinox xy plane is equator	not used	not used
orbital elements for boundary conditions		5	same as 2	same as 2	not used
		6	same as 3	same as 3	not used
		7	same as 4	same as 4	not used

2. Constants

The constants used in the program are listed in Table 2. Most of them were obtained from the American Ephemeris and Nautical Almanac. Mean Rate (ω), semi-major axis (D), and G are adjusted to satisfy $\omega^2 = G/D^3$.

TABLE 2. LUNAR ORBIT AND ASTRONOMICAL CONSTANTS

Eccentricity	=	.054900489
Mean Orbital Rate	=	13.17639 65268 °/day = ω
Incl. LOP to Ecliptic	=	5.1453964°
Incl. LOP to Lunar Equator	=	6.6804°
Incl. Ecliptic to Earth's Equator	=	23.44436° (Epoch of 1950)
Semi-major axis	=	384747.87 km = D
Gravitational Constant Times Total Mass	=	403505.3 km^3/sec^2 = G
Ratio Mass Moon/Total Mass	=	1/82.30 = M
Ref. Date. JD 2,439,000.5	=	Aug. 28,1965 0 hr. U.T.
Asc. Node at Ref. Date	=	69.3226°
Asc. Nodal Rate	=	- .0529539222°/day
Perigee at Ref. Date	=	56.5280°
Perigee Rate	=	.16435 80025 °/day
Mean Anomaly at Ref. Date	=	41.1600°
Mean Anomaly Rate	=	13.06499 24465 °/day

3. Data Entry

The procedures used in supplying controls and data to the program are shown in Tables 3 and 4. The controls shown in Table 3 are read by the main program and the data shown in Table 4 are read by the subroutine INPUT. The cards of Table 4 follow those of Table 3 with no separation in the deck.

TABLE 3. INPUT CONTROL CARD FORMAT

Card No.	Format	Fortran Symbol	Identification
1	6D12.8	XI(1)-XI(6)	XI are initial values for homogeneous solutions (there are 10 max.) in units desired.
2	4D12.8	XI(7)-XI(10)	XERR = controls NOSTEP if NOSTEP = 0
	E12.8	XERR	NOSTEP = No. of steps per time storage interval.
	3I4	NOSTEP,NINTP1, N(4)	NINTP1 = 1 + No. of time sections(max. 10) N(4) = Print control
3	6E12.8	RHOS(1)-RHOS(6)	RHOS are convergence tolerances on variables
4	6E12.8	RHOS(7)-RHOS(12)	
5	6(E9.3,I3)	TSUBT(I),KSUB(I)	Time (in hours) at section breaks in time history
		I = 1, NINTPI	Step numbers from beginning (max.value KSUB(NINTPI)) = 125

TABLE 3. con't.

Card No.	Format	Fortran Symbol	Identification
6	12I6	N(3),NREAD,NQ1 ISETUP,NDIF, JN(1) - (7)	N(3) = No. of iterations allowed. NREAD, NQ1, ISETUP not used. NDIF = No. of differences, 3 max. allowed (but see notes). JN(1) = No. of dimensions (2) = Flag for Special problems (3)-(7) = not used
7	6E12.8	SPARE (1) - (6)	Used to transfer information to subroutines XINM and those it calls (first time history section).
8	6D12.8	DPI (1) - (3) DPF (1) - (3)	Increments in initial, final positions;
9	6D12.8	DVI (1) - (3) DVF (1) - (3)	initial, final velocities;
10	4D12.8	DTI, DTF, DVARI, DVAR2	initial, final times; two other variables for cases using last time history.
	4I6	NCM,NICH(1)-(3)	NCM = total number cases based on the initial problem. (max is 30) NICH(1) = control for next case; NICH(2),(3) = not used.
11	36I2	NN(j),IDTI(J), IDTF(J),IDPT(J), IDDF(J),ICO(J) J=1, NCM	NN(J) = case no. (not used) IDTI(J) IDTF(J) IDPT(J) Integral multipliers IDDF(J) for increments ICO(J) These can be -9 to 99.
Extra cards as needed for integers			

TABLE 4. INPUT DATA FORMAT

Card No.	Format	Fortran Symbol	Identification
D1	2I6, 4I3, 2I6	LORM, IRAT, ICORC(I), IROTS(I), ICOEL, IMORTA	LORM= 1 Lunar unit = 2 metric units = 3 not specified IRAT= 1 real time= 2 artificial time ICORC, IROTS for specifying coordinate system (see Table 1) ICOEL = 1 moon's orbit circular = 2 moon's orbit elliptical IMORTA = moon's initial position given in mean (=1) of true (=2) anomaly.
	3E12.8	EXTRA(12) - (14)	not used
D2	6E12.8	PI(1) - (3)	Initial, final position vectors (If orbital elements: a, e, incl.)
D3	6E12.8	VI(1) - (3) VF(1) - (3)	Initial, final velocity vectors (If orbital elements: perigee, node, angle from node).
D4	6E12.8	TI, TF ATMA (1) - (3) EPOCH	Initial, final times'(Hours) N.B. TI must = TSUBT(1) but these do not have to be zero TF must = TSUBT (NINTP1) Moon's initial position: node, perigee, anomaly (Deg) Epoch of time scale for TI and TF in MJD for real time cases.
D5*	18I4	N1, NC, M(1)-(15)	N1= Number of variables NC = 0 M(1) = no. of points to be connected by linear segments for variable numbered I

TABLE 4. INPUT DATA FORMAT con't.

Card No.	Format	Fortran Symbols	Identification
D6* Extra cards as needed	12D6.3	Z(K), W(K)	Z(K), W(K) = (time, value of variable). Limit is 50 pairs

*When using linear segments as the initial estimate of the trajectory.

4. Program Controls

Use of the program controls and the data input procedure is described below. Many of the storage dimensions of the variables are those required by subroutine QASLIN which can manage a total of 12 variables having 10 initial boundary conditions to be found. In the two-impulse problem there are either 6 variables with 3 unknown initial boundary conditions for a three-dimensional case or 4 variables with 2 unknown initial boundary conditions for the two-dimensional case. The numbering of the variables then proceeds as $\dot{x},\dot{y},\dot{z},x,y,z$ or $\dot{x},\dot{y},x,y$ for the three and two-dimensional situations. The data and controls along with the boundary conditions in the rotating system are printed on the first two pages of output. A sample is included as Figure 3. The card numbers 1,2,3,4, refer to the cards D1, D2, D3, D4 of Table IV.

A list of variables and their definitions follows:

XI(I)	These are the values V_1, V_2, V_3 etc. of the non-zero initial values used for the series of homogeneous solutions as described in the text following Equation 14.
XERR	The step-size or equivalent, NOSTEP, is determined from the 5th root unless NOSTEP is given directly.
NOSTEP	The number of integration steps per time storage interval. This can be as large as desired but a maximum of 3 is suggested since the second order interpolation on the previous time history uses values at the storage points.

INPUT FOR JUL 28, 1966

CARD	COLS.		VALUE		VARIABLE
1	6		2		UNITS 1= LUNAR, 2= METRIC, 3= ALTERNATE
1	12		1		TIME 1= REAL, 2= ARTIFICIAL
1	15,18		1 2		COORD. CENTER 1=EARTH, 2=MOON, 3=BARY
1	21,24		2 2		ROTAT. SYSTEM 1=STAND., 2=SYS1, 3=SYS2
					*** ORBITAL ELEMENTS IN--5 = SYS1, 6 = SYS2
1	30		1		LUNAR ORBIT 1=CIRCULAR, 2=ELLIPTICAL
1	36		1		ANOMALY FLAG 1=TRUE, 2=MEAN
2	1-36	-4.50310D 03	-4.82900D 03	0.00000D-39	INITIAL POSITION VECTOR
2	37-72	1.20000D 03	1.60000D 03	2.00000D 01	FINAL POSITION VECTOR
3	1-36	4.20200D 00	-4.11000D 00	0.00000D-39	INITIAL VELOCITY VECTOR
3	37-72	-1.20000D 00	-1.00000D 00	0.00000D-39	FINAL VELOCITY VECTOR
4	1-12		0.00000D-39		INITIAL TIME (HRS.)
4	13-24		6.98000D 01		FINAL TIME (HRS.)
4	14-36		-0.00000D-39		*MOON'S POSITION, NODE
4	37-48		-0.00000D-39		*MOON'S POSITION, PERIGEE
4	49-60		-0.00000D-39		*MOON'S POSITION, ANOMALY
4	61-72		4.376450D 04		**EPOCH (MJD)

* FOR ARTIFICAL TIME ONLY
**FOR REAL TIME ONLY
*** P AND V VECTORS CONTAIN A,E,I,SOMEGA,COMEGA,PHI

REAL TIME CASE, REFERENCE EPOCH/DEPARTURE TIME/ARRIVAL TIME
JULIAN DATE 24 43764.5000 IS SEPT. 13, 1978 0.000 HOURS U.T. OR 1900 + 78.699520 YEARS
JULIAN DATE 24 43764.5000 IS SEPT. 13, 1978 0.000 HOURS U.T. OR 1900 + 78.699520 YEARS
JULIAN DATE 24 43767.4082 IS SEPT. 15, 1978 21.797 HOURS U.T. OR 1900 + 78.707482 YEARS

CONSTANTS ARE IN METRIC UNITS, THEY ARE

ECEN	=	5.49005E-02	ECON	=	1.05649E 00	XNO	=	1.31764E 01	XIE	=	2.34446E 01
XIL	=	5.14540E 00	XLE	=	6.68040E 00	TCON	=	4.34836E 00	DD	=	3.84748E 05
MU	=	1.21286E-02	REMJD	=	3.95005E 04	RNODE	=	6.93226E 01	DNODE	=	-5.29539E-02
RPER	=	5.65280E 01	DPER	=	1.64358E-01	RM	=	4.11600E 01	DOTM	=	1.30650E 01
GXM1	=	3.98611E 05	GXM2	=	4.89394E 03	B1	=	4.66644E 03	B2	=	3.80081E 05

SPARE(1-6)=DATA FOR XIN /DPI,DPF/DVI,DVF/DTI,DTF,DVAR1,DVAR2,NCM,NICH
0.100000E 01 0.200000E 01 0.200000E 02 0.100000E 02 0.850000E 00 0.100000E-02

SID 66-1224

Figure 3 - Computer Program Output

```
 0.1000000D 02    0.0000000D-38    0.0000000D-38    0.0000000D-38    0.1000000D 03    0.0000000D-38
 0.0000000D-38    0.0000000D-38    0.0000000D-38    0.0000000D-38    0.0000000D-38    0.0000000D-38
 0.5000000D 00    0.5000000D 00    0.3000000D 02    0.0000000D-38       3       1   2   3
82  0  0  0  0  0   0  0  0  0  1  0   3  0  0  1  0  0
```

THE BOUNDARY CONDITIONS ARE

	TIME	M.ANOM.	TRUNOM	THETA	E-M DIST.
INIT.	0.0000D-39 HRS.	3.102878D 02 DEG.	3.102878D 02 DEG.	1.067638D 03 DEG.	3.847479D 05
FINAL	6.9800D 01	3.486091D 02	3.486091D 02	1.105960D 03	3.847479D 05

INIT. POSITION VECTOR =	-8.031334D 03	-5.681077D 03	-0.0000000D-39
FINAL POS. VEC.	3.818607D 05	9.132782D 02	2.0000000D 01
INIT. VELOCITY	4.969336D 00	-3.106182D 00	0.0000000D-39
FINAL VEL.	-1.514230D 00	-3.785527D-01	-0.0000000D-39

THE CONTROLS ARE

AT STEP	1	31	56	66	76	86	96	105	125
T(HRS.)	0.00	0.50	2.00	4.50	14.50	54.50	68.00	69.30	69.80
(LORMU)	0.000D-39	1.800D 03	7.200D 03	1.620D 04	5.220D 04	1.962D 05	2.448D 05	2.495D 05	2.513D 05

INTEGERS NOSTEP,	NINTP1,	PRINT ,	MAX.ITR,	NREAD,	NQ1,	ISETUP,	IMAX,	NDIF,	NO.DIM.,	JN(2,7)			
2	9	1	6	1	1	1	125	3	3	1	2	2	1	2

12 RHOS,10XI, XERR

1.000000E-05	1.000000E-05	1.000000E-03	1.000000E-03	1.000000E-03	1.000000E-03
0.000000E-39	-0.000000E-39	-0.000000E-39	-0.000000E-39	-0.000000E-39	-0.000000E-39
1.000000D-01	1.000000D-01	1.000000D-01	1.000000D 00	1.000000D 00	1.000000D 00
0.000000D-39	0.000000D-39	0.000000D-39	0.000000D-39	0.000000E-39	

AT START MOON SECTION RESULTS ARE /SP,EE,SA,HP,TT/ APH1,AA1,X,Y,EM/RM2,RM3,SF2,SF3,SPM/SAM,PH3,

1.1600127D 04	9.7890379D-01	2.7786491D 05	3.4539473D 05	2.5128000D 05
1.0360587D 00	3.4906585D-01	3.0345629D 05	5.2222320D 04	1.3283131D 00
2.0000000D 03	9.2728548D 04	2.9968083D-01	2.3688377D 00	4.5382223D 03
-5.9368523D 03	2.5433707D 00	1.2128563D-02	4.0350530D 05	8.4000000D 01

Figure 3 - Computer Program Output con't.

NINTP1	The total time of the trajectory can be divided into as many as 9 sections in each of which the step-size interval is constant. NINTP1 number of such sections plus 1.
N(4)	Print control (each integer above 0 adds the items listed to the output) 0 = Final solution is only printed 1 = Time history at end of each iteration 2 = Partial integral (P) and H's during integration
RHOS(12)	The values of the differences of the variables to be compared with the vector ξ. Convergence is said to have occured when for every component $\xi \leq \rho$. The units must correspond to those computed by the program as no conversions are used.
TSUBT(I), KSUB(I)	The boundaries of the time storage sections and the corresponding step numbers (times in hours).
N(3)	The maximum number of iterations allowed for the QASLIN routine.
NREAD,NQ1,ISETUP	Not used.
NDIF	Number of differences used in the Adams-Moulton integration (3 maximum allowed). If larger than 3, 3 is assumed and 4th order Runge-Kutta-Gill integration will be used for NDIF steps before the program switches to the

	Adams-Moulton integration for the remainder of the time.
JN(1)	Number of dimensions of problem (2 or 3).
JN(2)	1-normal problem 2-special problem setup. (Dummy at present)
JN(3) - (7)	Not used
SPARE(1) - (6)	Used for transfer of information to XINM and the subroutines it calls. (The initial time history section).
SPARE(1)	If negative the linear segmented input routine is called. If positive, used to give conic center of initial point when barycentered system is used for initial conditions, i.e., when ICORC(1) = 3.
SPARE(2)	Used to give conic center of final point when barycentered system is used for final conditions; i.e., when ICORC(2) = 3.
SPARE(3)	Angle of perigee of earth centered ellipse (measured c.c.w. from direction opposite the moon) (see Figure 4).
SPARE (4)	Angle of perilune of moon centered conic, measured c.c.w. from X axis. (see Figure 4).
SPARE(5)	RLIM = SPARE(5)*D (see Figure 4).
SPARE(6)	Not used.

DPI(K), DPF(K) DVI(K), DVF(K) DTI, DTF DVAR1, DVAR2	Increments for changes in boundary conditions for new cases based on the previous case. For each new case each variable new value = old value plus increment *ID XX (IDPI is used for both DPI and DVI and similarly for IDPF), DVARI is increment in lunar position, DVAR2 not used, K = 1, 2, 3
NCM	Maximum number of cases based on a given solution (maximum is 30).
NICH(1)	Control for new case 1 = new data and new controls 2 = new data only 3 = exit
NICH(2), (3)	Not used
NN(J)	Not used except that for NN(NC) = 81, 82 ICOEL is set to 1, 2.
IDTI, IDTF, IDPI, IDPF, ICO	All dimensioned 30, as is NN. These are integral multipliers for increments in corresponding quantities and they can be from -9 to 99.
N1	The number of variables of the problem.
NC	This must equal 0. Other values are for a capability of the subroutine XILS not now required by this program.
M(I)	The number of points that determine the linear segments for variable numbered I. This is one more than the number of segments desired.

Z(K), W(K)	(Time, Value) pairs. Note that the time must be in the units called for by the program and that the pairs for each variable are grouped together, i.e. the first M(1) pairs refer to the M(1)-1 sections for the variable μ or $\dot{x}$)

5. Time History Storage

At the moment the maximum number of storage points is set at 125. Since the QASLIN integration procedure is capable of handling a change in step-size it is permissible to divide the total time and the 125 points into sections of constant step-size as in Figure 4a or 4b, page 37, Appendix A. This is desirable so that when near the earth or moon a small step-size can be used for accuracy because the forces of attraction are large and vary greatly over short distances. Over the intermediate distances longer step-sizes will give equivalent accuracy. The optimal use of the available steps is a subject for study after the program is running. The total number of steps might be increased somewhat but this consideration, as noted above, will require some streamlining of the program so as not to exceed core or the use of an overlay maneuver on the computer. Very large increases in step-size between sections has been found unsatisfactory in that the extrapolation for new large intervals is very much less accurate than the computation for the previous steps. It is best to keep the step-size change to a factor of two to four.

6. Initial Time History

In order to begin the quasilinearization process it is necessary to generate an initial guess for the time history of all the variables (X). In many cases this can be very crude but for highly sensitive and extremely non-linear problems the first guess may have to be carefully made in order to obtain convergence on the desired solution. Two-impulse transfer in the three-body problem presents such a situation if the trajectory sought is to transfer from the space near one body to that near the other.

The motions envisaged for study so far have been those fairly close to the lunar orbit plane (LOP). The motion out of the plane has been assumed to be linear and decoupled from the motion in the LOP, but a sinusoidal form could be utilized with very little additional programming if it is needed.

Three approaches for obtaining a first time history in the LOP have been utilized in this study. The first was an attempt to find a simple two-for-one Lissajous figure with variable amplitude to obtain an approximate trajectory. This form did succeed in the case tested but required several iterations before the trajectory was really close to convergence. In addition, it was felt that because one has to put in arbitrary variations in the velocity formulae to approximate the lunar trajectory velocities more realistically, the technique may not be very satisfactory.

With the hope of reducing the number of iterations required for convergence, patched conic procedures were then setup for the first time history along with controls so that the various types of Earth to Moon, Earth-Earth, Moon-Moon and Moon to Earth transfers could be studied.

In addition a linear segmented time history program allowing up to 50 pairs of points to produce linear segments for all variables was available and it was adopted for use in this program. All three schemes have been made to yield satisfactory first time histories, however, because of its artificiality the first scheme has, for the present at least, been dropped from the program.

Only one comparison between linear segmented and patched conic cases has been made so far and this was for an Earth to Moon transfer requiring 149 hours. The linear segments for the trajectory were chosen to represent as closely as possible the results from a portion of a run made using the Fehlberg three-body problem integration program developed at MSFC. Eight iterations were needed to accomplish convergence to a vector of values .00001 ld/ut, .00001 ld/ut, .000001 ld, .000001 ld. The very same problem using the patched conic routine likewise required 8 iterations to the same degree of convergence and it did not require any previous knowledge of the trajectory except the general shape, i.e. that it is retrograde around the moon. Consequently, it is concluded that the patched conic technique is the most effective one to use.

The patched conic scheme has been programmed for Earth to Moon transfers with retrograde motion around the Moon, and for Earth-Earth transfers in which both the initial and final points are on orbits around the Earth. In all cases the motion is considered to be on a conic section in the rotating system, that is, the computations are performed in the standard rotating system and the fact that it is not inertial is ignored.

The specific details to be supplied to the patched conic routine for Earth to Moon trajectories are the pericenter angles A_1,A_2, and RLIM as

shown in Figure 4.

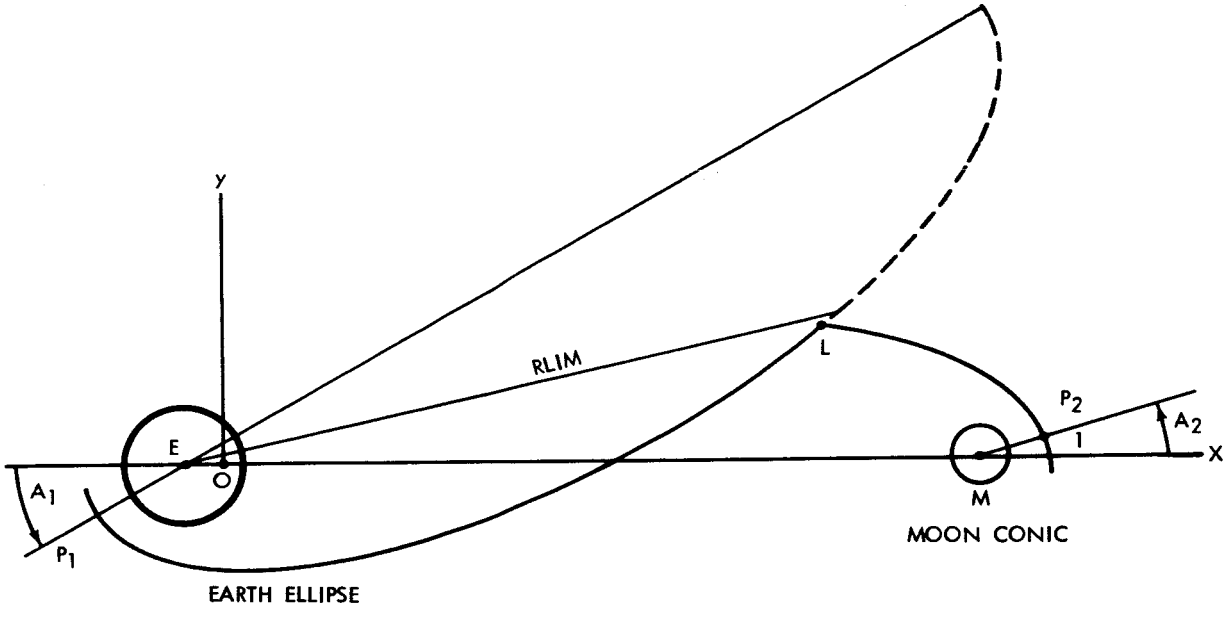

NOTE: P_1 AND P_2 ARE PERIGEE AND PERILUNE

Figure 4. Patched Conic Geometry for Earth to Moon Transfers

These quantities are supplied through the use of SPARE(1) as follows:

A_1 = SPARE(3) = Angle of Perigee (P_1) in Deg.

A_2 = SPARE(4) = Angle of Perilune (P_2) in Deg.

RLIM = SPARE(5)*D

The semi-major axis of the Earth section conic is chosen by means of the formula

$$a = (.712 - (TF - TI - 80)* .001.)*D \text{ l.u.}$$

This was developed to give a reasonable value for an eighty hour trip

to the Moon and slightly higher semi-major axes for shorter trips. This scheme was chosen rather than one assuming that the period should be proportional to the trip time, since this calls for a variation in "a" of the proper direction as far as energy is concerned. Finally the eccentricity is determined from the initial point since the true anomaly is known.

The Earth section conic is followed until the distance from the Earth exceeds the value RLIM. Then the previous point (L) and the final one, A = B_T are used to determine the lunar conic. Since perilune has been chosen the lunar conic is now fixed and its elements are determined. The program can manage either an ellipse, or a hyperbola for this conic. The mean anomaly rate is taken to be the mean anomaly difference between L and A divided by the remaining time to go, thus assuring arrival at A at the proper time. Although this orbit may be traversed at an improper rate, the velocity time history contains the velocity components corresponding to the proper rate.

7. Subroutine QASLIN

A double precision subroutine for managing a quasilinearization operation as outlined in Section II above has been developed by McCue and Radbill (Ref. 2). The details of its use in the present program are given in Section III (Table 3) and Section IV under the items listed for the first six control cards.

8. Program Output

As shown in Fig. 3 , the output consists first of the input data in its entirety and the boundary conditions which include the initial and final positions of the Moon in its orbit as well as the boundary values for the departure point and arrival point of the space ship in the rotating barycenter system.

In case the initial time history is generated by using conic sections, the orbital elements of the conics are printed. The next item of output is the initial time history (if called for) which is printed by QASLIN according to the value of N(4) as explained in Section IV (see also Table 3, card 2).

Then follow the values (at $t = 0$) of the Jacobian (J), the derivatives (g_i), and six other quantities including the distances to the Earth and Moon printed by the subroutine JACOB which computes them. This has served as a means of checking the computation of these quantities and it remains in the program.

The amount of output per iteration is controlled by N(4) as is explained above in Section IV except that when integrating the equations of motion with the converged values for the initial velocity, the print of the time history is produced by the subroutine JACOB. Whenever a time history is printed (except for the initial time history) the value of the Jacobi integral (Eq. 7) for restricted three-body problem is computed and printed. The degree to which this value stays constant (when $\dot{\omega} = 0$) is an indication of the accuracy of the integration techniques.

The minimum output at the conclusion of an iteration consists of a matrix giving the equations to be solved for c_1, c_2, c_3 (of Eq. 14), the

values of c_1, c_2, c_3 and the vector ξ. In addition, for this problem the impulses at both ends are determined and printed each time an output time history of the variables is called.

The details of the output can be varied by controls in the various subroutines as is indicated by the current usage and the existence of unused items on the data cards and in the labelled common regions of the program. When the applications of the program are more fully developed an output plan giving only the needed details can be used.

PRELIMINARY RESULTS

Two different transfer orbit cases have been used so far in testing the program. The first is a case using lunar units, the boundary conditions for which were taken from two points along a periodic trajectory computed with the double precision Fehlberg program. The second is a 69.8 hour flight from very near the earth to very near the moon using real time and either two or three dimensions. The input data of Figure 3 are for this second case in three dimensions.

As has been indicated the variation in the value of the Jacobi integral along the trajectory may be taken as a measure of the accuracy of the trajectory. The values found for the final time history as given by the quasilinearization technique and those found by direct integration of the original equations with the initial conditions found agree to the accuracy of the comparisons given below and thus no distinction between them is made. In Table 5 are shown the results for two runs using the Fehlberg case (Case 1). It can be seen that the very large increase in the time step-size in the first of these runs leads to a substantial discontinuity in the value at the change over point. The second run shows that this difficulty has been almost completely corrected by keeping the step-size ratio under 4.

In order to maintain a constant value of the integral near the Earth or Moon it is clear from this table and other similar cases that a small step-size is needed. In this case also it is seen that the integration scheme apparently affects the variation when near the Earth. The step-

Table 5. Behavior of Jacobi Integral Case 1
(Value from Fehlberg run 2.08602504 $(ld)^2/(ut)^2$

Integration Technique*	Time Step Used Number Steps	Value of Integral at boundary steps (with note) $(ld/ut)^2$	Distance to Earth (/and Moon) ld
Runge Kutta Gill	9 min for 20 steps	2.049 522 (high 27 low 05) 2.049 545	.0617 .0860
	220 min for 40 steps	2.085 619 (rapid rise then nearly constant) 2.086 201	.1935 1.210/.215
Adams-Moulton	7.5 min for 24 steps	2.087 435 (high 7 810 low 4 291) 2.086 036	.0617 .0875
	16.8 min for 25 setps	037 (low 020) 023	.0973 .270
	60 min for 20 steps	024 029	.291 .584
*(See note on NDIF in Section 4)	120 min for 20 steps	029 029	.600 .943/.618
	210 min for 20 steps	029 030	.966/.602 1.203/.236
	38.4 min for 15 steps	030 2.086 030	 1.210/.215

sizes of the second run in Table 5 appear to be satisfactory for the intermediate regions.

In the case of the second run of Table 5, the convergence criterion, ξ, for the difference between successive iterations was set at 10^{-5} ld/ut for each velocity component and at 10^{-6} ld for each position component. Convergence was obtained in 7 iterations, each of which required very nearly .15 minute of computer time. In addition about .17 minute was required for the initializing process including the generation of the initial time history as a patched conic. Table 6 shows the behavior of the total impulse value and the convergence measure for the last three iterations. The convergence measures given are the larger of the two velocity and position components of the vector ξ. It can be seen that the convergence rate is extremely good for the last few iterations and that the values obtained for the impulse likewise show strong convergence to a final value.

The computer time used is one of the output quantities at each iteration and thus it is possible to indicate how the computer time is used. Preliminary time studies showing several runs of the two tests cases are given in Table 7 along with some details which influence the time. There are included three runs based on the runs directly above in the table in which some moderate change in a boundary condition is made and for which the previous time history is modified for the new initial time history. As expected this new case is rapidly solved. Thus, the procedure can be used for impulsive transfer studies and can be developed into a search program for finding optimal impulsive transfers in the three-body problem.

TABLE 6. IMPULSE AND CONVERGENCE MEASURE

Iteration Number	Total Impulse (ld/ut)	Convergence Measure	
		Vel.(ld/ut)	Pos.(ld.)
5	.0276 4243 3894	2.2×10^{-2}	2.9×10^{-4}
6	.0276 4094 2633	9.8×10^{-5}	9.5×10^{-7}
7	.0276 4094 2084	5.4×10^{-9}	1.42×10^{-10}
(1 ld/ut = 1.024km/sec)			

Table 7. Computer Times

Case	Method for Initial Time History	No. of Dimen.	Output*	No. of Storage Points	Time at First Iter. (min)	Time per Iteration	No. of Iteration	Time at End (min)
Fehlberg Comparison	Lin.Segments	2	F	125	.200	.200	6	1.333
	Prev. Case	2	F	125	.184	-	1	.334
	Patch. Conic	2	P	125	.150	.167	8	1.383
	Prev. Case	2	P	125	.133	.158	3	.584
Earth to Moon in 69.8 hours	Patch. Conic	3	P	125	.267	.267	5	1.555
	Patch. Conic	3	F	91	.333	.308	3	----**
	Patch. Conic	2	P	125	.167	.154	5	.933
	Prev. Case	2	P	125	.134	.158	3	.567

**Not run to end

P* = Partial - Includes Final Time Histories

F* = Full - Includes H & P Vectors at all Points

CONCLUSION

A double precision computer program which uses quasilinearization to find impulsive transfers between given terminals in the three-body problem has been shown to give accurate solutions with considerable speed. However, there are still three items to be completed before the program can be generally useful: (1), further tests will be needed to determine more precisely the controls and limits needed to produce results satisfying a given accuracy requirement; (2), the development of initial time history sections for Moon to Earth trajectories and for lunar orbit changes is needed, and (3), the management of the entire initial time history section for the first case of a series should be controlled by means of an overlay process on the computer, thus, allowing an expansion in the number of points that can be stored for the time history.

REFERENCES

1. McGill, R. and Kenneth, P., "Solution of Variational Problems by Means of a Generalized Newton-Raphson Operator," AIAA J., 2, pp. 1761-1766 (October 1964).
2. Radbill, J.R., and McCue, G.A., "QASLIN--A General Purpose Quasilinearization Program," North American Aviation, Inc., SID 66-394 (June 1, 1966).